Astronomical & Astrophysical Transactions

The Journal of the Eurasian Astronomical Society

THE RELATION BETWEEN THE SURFACE BRIGHTNESS AND THE DIAMETER FOR GALACTIC SUPERNOVA REMNANTS

O. H. Guseinov [a]; A. Ankay [b]; A. Sezer [a]; S. O. Tagieva [c]
[a] Department of Physics, University of Akdeniz, Antalya, Turkey.
[b] Bogazici Uni.--TUBITAK, Feza Cicersey Institute, 81220 Cengelkoy, Istanbul, Turkey.
[c] Physics Institute, Academy of Science, Baku 370143, Azerbaijan Republic.

PLEASE SCROLL DOWN FOR ARTICLE

Taylor & Francis
Taylor & Francis Group

THE RELATION BETWEEN THE SURFACE BRIGHTNESS AND THE DIAMETER FOR GALACTIC SUPERNOVA REMNANTS

O. H. GUSEINOV [a,*], A. ANKAY [b,†], A. SEZER [a,‡] and S. O. TAGIEVA [c,¶]

[a]*Department of Physics, University of Akdeniz, Antalya, Turkey;*
[b]*Bogazici Uni.—TUBITAK, Feza Cicersey Institute, 81220 Cengelkoy, Istanbul, Turkey;*
[c]*Physics Institute, Academy of Science, Baku 370143, Azerbaijan Republic*

In this work, we have constructed a relation between the surface brightness (Σ) and diameter (D) of Galactic C- and S-type supernova remnants (SNRs). In order to calibrate the Σ–D dependence, we have carefully examined some intrinsic (*e.g.* explosion energy) and extrinsic (*e.g.* density of the ambient medium) properties of the remnants and, taking into account also the distance values given in the literature, we have adopted distances for some of the SNRs which have relatively more reliable distance values. These calibrator SNRs are all C- and S-type SNRs, *i.e.* F-type SNRs (and S-type SNR Cas A which has an exceptionally high surface brightness) are excluded. The Σ–D relation has 2 slopes with a turning point at $D = 36.5$ pc: Σ(at 1 GHz) $= 8.4^{+19.5}_{-6.3} \times 10^{-12}$ $D^{-5.99^{+0.38}_{-0.33}}$ W m^{-2} Hz^{-1} ster^{-1} (for $\Sigma \leq 3.7 \times 10^{-21}$ W m^{-2} Hz^{-1} ster^{-1} and $D \geq 36.5$ pc) and Σ(at 1 GHz) $= 2.7^{+2.1}_{-1.4} \times 10^{-17} D^{-2.47^{+0.20}_{-0.16}}$ W m^{-2} Hz^{-1} ster^{-1} (for $\Sigma > 3.7 \times 10^{-21}$ W m^{-2} Hz^{-1} ster^{-1} and $D < 36.5$ pc). We discussed the theoretical basis for the Σ–D dependence and particularly the reasons for the change in slope of the relation were stated. Added to this, we have shown the dependence between the radio luminosity and the diameter which seems to have a slope close to zero up to about $D = 36.5$ pc. We have also adopted distance and diameter values for all of the observed Galactic SNRs by examining all the available distance values presented in the literature together with the distances found from our Σ–D relation.

Keywords: Supernova remnant, neutron star, distance.

1 INTRODUCTION

In the last 40 years it is known that there is a rough relation between the surface brightness value (Σ) in the radio band and the diameter (D) of Supernova remnants (SNRs) (Shklovsky, 1960; Poveda and Woltjer, 1968; Clark and Caswell, 1976; Caswell and Lerche, 1979; Milne, 1979; Lozinskaya, 1981; Sakhibov and Smirnov, 1982; Allakhverdiev *et al.*, 1983a,b; Huang and Thaddeus, 1985; Allakhverdiev *et al.*, 1986c; Green, 1984; Li and Wheeler, 1984; Mills *et al.*, 1984; Berkhuijsen, 1986; Case and Bhattacharya, 1998).

If the whole SNR is bright and extends in a medium with roughly homogenous density then both its radio flux, F (mostly at 1 GHz), and its angular diameter, θ can be measured

---

precisely. But in most of the cases, as the radiation coming from some parts of the SNR has low intensity the whole of the shell can not be observed (Green's catalog 2001; Caswell and Lerche, 1979; Milne, 1979; Allakhverdiev et al., 1986b). Also in some cases, as the SNR is projected onto a HII region its angular size and its flux can not be measured precisely (Weiler and Panagia, 1978; Israel, 1980; Blandford and Cowie, 1982; Allakhverdiev et al., 1983b; Mills et al., 1984; Allakhverdiev et al., 1986a). As well known:

$$\Sigma \propto \frac{F}{\theta^2} \propto D^{-n} \tag{1}$$

If only the bright part of the SNR is seen then the Σ of the remnant will be overestimated, because the measured value of θ will be smaller than the real value of the angular size. What will be the effect of such an error on the distance value found from the Σ–D relation? From Eq. (1)

$$D \propto \frac{\theta^{2/n}}{F^{1/n}} \tag{2}$$

Using Eq. (2) we can find a relation between distance (d), θ and F:

$$d = \frac{D}{\theta} \propto \frac{\theta^{(2-n)/n}}{F^{1/n}} \tag{3}$$

If $n = 2$ then overestimation (underestimation) of the $\Sigma(\theta)$ value has no effect on estimation of the distance value. If $n > 2$ then overestimation (underestimation) of the $\Sigma(\theta)$ value leads to overestimation of the distance value and the degree of overestimating the distance value increases with n. If $n < 2$ (which is not the case for the Σ–D relation as we will see below and this is known from various previously suggested Σ–D relations) the distance value will be underestimated in the case of underestimating (overestimating) the $\Sigma(\theta)$ value. An HII region projected onto the SNR may lead to overestimation of the flux value of the SNR and in such a case, from Eq. (3), there will be an underestimation of the distance value.

Observationally, SNR distances are found in general using the shift value of 21 cm HI line and galactic rotation models. By this method, for some of the SNRs (for which the radial velocity is large enough) distances can be found with percentage errors of about 30%–50% at best. The error increases in the vicinity of longitudes $l = 0°$ and $l = 180°$ and when a SNR is in or close to the galactic center direction 2 values of distance, which are very different from each other, are found. If the SNR is found to be related with some other objects (which are located relatively close to the Sun) its distance can be determined more precisely, but in any case, error in the distance value is not smaller than about 20–30%. So, in order to find distances of the SNRs, particularly the ones located at > 3–4 kpc, Σ–D relation is needed.

In Figure 1 we see that the dispersion of the positions of the calibrators (the SNRs which are used to calibrate the Σ–D relation) from the Σ–D relation is very high. The reasons for such high dispersions, in other words, the reasons for the Σ–D relation being not very reliable are discussed in detail by Allakhverdiev et al. (1986b).

The increase in number of reliable calibrators do not decrease the dispersions much (Allakhverdiev et al., 1986b). The reasons for such dispersions are:

(1) Explosion energies of supernovae (SNe) vary in a wide range, about 3 orders of magnitude (e.g. kinetic energy of Crab SNR is $\sim 10^{49}$ erg, Sollerman et al., 2000, whereas kinetic energy of Cas A SNR is $> 10^{51}$ erg, Vink et al., 1998; Wright et al., 1999). So, it is important for con-
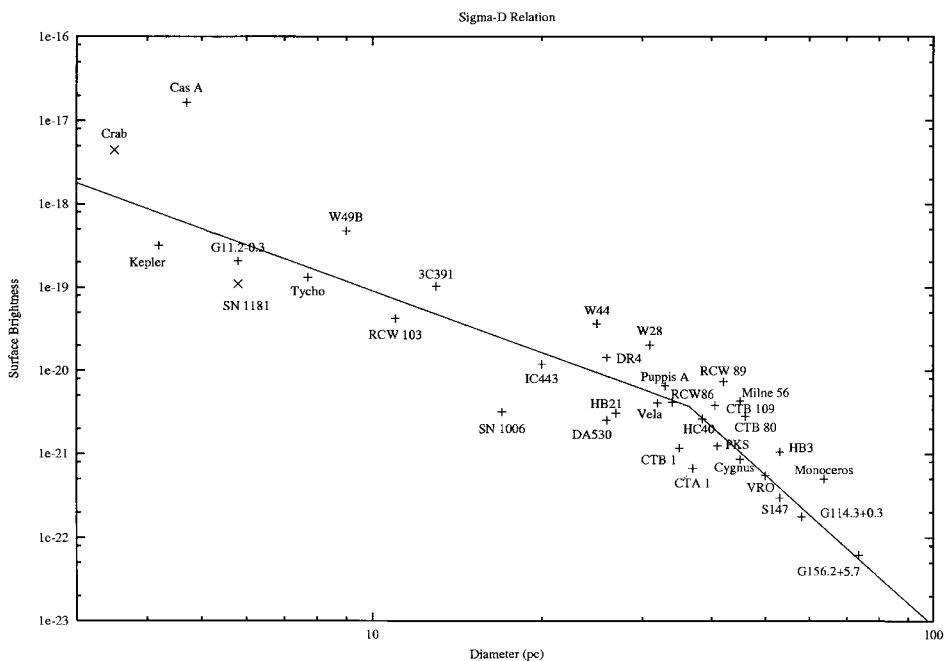
FIGURE 1   Surface brightness ($W\,m^{-2}\,Hz^{-1}\,sr^{-1}$) versus diameter (pc) diagram (see text).

structing the Σ–D relation to examine the differences between the energies of calibrator SNRs. For example, SNR G11.2−0.3 has an explosion energy $E \sim 10^{48}$–2.4×10^{49} erg (Bandiera *et al.*, 1996), whereas SNR G320.4−1.2 has $E \sim (1$–$2) \times 10^{51}$ erg (Gaensler *et al.*, 1999b). For SNR G109.1−1.0 the energy may even be larger: $E \sim 10^{51}$–10^{52} (Morini *et al.*, 1988).

(2) Surface brightness of a SNR depends on density of the interstellar medium in which it expands as well as the kinetic energy of the expanding matter. The denser the medium is the higher the surface brightness will be under similar velocities (it must be noted that the lifetime of a SNR, in other words the time needed for the SNR's surface brightness to drop below a certain value, directly depends on the density of the medium and the SN explosion energy).

(3) If there is a very active neutron star (NS) within the SNR which has a significant contribution to the SNR's energy, then the central part of the SNR can be much more bright.

There are 231 SNRs observed up to date (Green, 2001). 155, 18 and 8 of them are S, C and F-type, respectively. For 50 of them type is either not known or not reliable. Naturally, number of SNRs increase as the SNRs are examined more precisely and as some new SNRs are found, but the increase in their number does not significantly change the ratio between different morphological types of SNRs. As S and C-type SNRs have very different characteristics compared to F-type SNRs and as there are not many F-type SNRs, Σ–D relation is constructed only for S and C-type SNRs and F-type remnants are not used as calibrators. As C-type SNRs are not different from S-type SNRs with respect to their energy and birth sites and because of the radiation coming from the plerionic part often being very low compared to the radiation coming from the shell, they can be used as calibrators for Σ–D relation. In general, for C-type SNRs the radiation coming from the shell is larger than the radiation coming from the plerionic part. But it must be noted that among the SNRs with $D > 20\,pc$ the largest surface brightness values belong to the remnants W44, W28, RCW 89 and Milne 56 all of which are C-type SNRs.

2 SUPERNOVA REMNANTS AS CALIBRATORS

We examined the SNRs given in Green (2001) and also some recently found SNRs with at least one observationally found distance value collecting radio, X-ray, and in some cases optical data of the SNRs. Among these SNRs we chose the ones with reliable distance values as calibrators to construct the Σ–D relation. The data of these SNRs which are essential for the Σ–D dependence are responsible for the deviations from the Σ–D dependence are given below (Section 2.3). The calibrator SNRs are presented in the order of their galactic longitude (l) values and the calibrators with relatively more reliable distance values are presented before the calibrators with relatively less reliable distance values. All the calibrators are represented with asterisk (*) sign in Table I. In Table I, we represented the distances calculated using the Σ–D relation, the adopted distance values, the values of surface brightness and luminosity at 1 GHz for all of the Galactic SNRs. While adopting the distances of the SNRs which are not calibrators, we have taken into account the distance values given in the literature, the data about the surrounding matter, the Galactic coordinates, and the Σ–D distances. The data and the references about the SNRs which were not adopted as calibrators, were taken from Tagieva (2002). In Table I, PSRs (P), X-ray pulsars (XP), pulsar wind nebula (PWN), anomalous X-ray pulsars (AXP), dim radio quiet neutron stars (D) connected to SNRs are also shown in the third column.

2.1 Abbreviations for SNR Data

1. SNR type: S-Shell, C-Composite
2. Angular size for the shell and the plerionic part as a whole: θ (arcmin)
3. Radio spectral index for the shell and the plerionic part separately and for the whole SNR: α
4. Distance: d (kpc)
5. Column density of neutral hydrogen (HI): N_{HI} cm^{-2}
6. Interstellar optical absorption: A_V (mag)
7. Radio flux at 1 GHz: F_1 (mJy)
8. Flux in X-ray band: F_x (erg/cm^2 s)
9. Temperature of plasma in the shell: kT (keV)
10. Velocity of shock front or expansion velocity: V (km/s)
11. Surface brightness: Σ (W m^{-2} Hz^{-1} sr^{-1})
12. Radio luminosity at 1 GHz: L_1 (Jy erg s^{-1})
13. Luminosity in X-ray band: L_x (erg/s)
14. For density of the SNR environment and types of clouds:
    (a) Molecular cloud: MC
    (b) Maser source (formed due to interaction between SNR and MC): MS
    (c) Dust cloud: DC
    (d) Neutral and ionized hydrogen clouds: H I and H II clouds
    (e) Number density of particles in front of SNR, in shell, in plerionic part, in different types of clouds and filaments: n (cm^{-3})
15. Kinetic energy of SNR: E_k (erg)
16. Explosion energy of SN: E (erg)
17. Age of SNR: t (kyr)
18. X-ray radiated mass: M_x (M$_\odot$)
19. Ejected mass: M_{E_j} (M$_\odot$)
20. Swept-up mass: M_s (M$_\odot$)
21. Total mass: M (M$_\odot$)
22. Magnetic field in the shell: B (Gauss)

TABLE I   Data of Galactic SNRs.

l,b	Name	Type	Σ	$d_{\Sigma-D}$ (kpc)	$D_{\Sigma-D}$ (pc)	d_{ado} (kpc)	D_{ado} (pc)	L (erg/s)
0.0+0.0	SgrAE	S	1.720E−18	3.61	3.05	8.5	7.2	3.12E+35
0.3+0.0		S	2.759E−20	5.10	16.25	5.4	17.2	2.77E+34
0.9+0.1		C(PWN)	4.233E−20	5.90	13.66	8	18.5	4.98E+34
1.0−0.1		S	3.527E−20	6.35	14.71	6.4	14.8	2.66E+34
1.4−0.1		S	3.010E−21	12.97	37.72	13	37.8	1.46E+34
1.9+0.3		S	6.271E−20	33.75	11.65	20	6.9	1.04E+34
3.7−0.2		S	2.248E−21	10.99	39.6	11	39.6	1.20E+34
3.8+0.3		S?	1.858E−21	7.81	40.88	7.8	40.8	1.05E+34
4.2−3.5		S	6.143E−22	6.04	49.18	6	48.8	4.98E+33
4.5+6.8*	Kepler	S	3.177E−19	7.14	6.04	4.8	4.1	1.89E+34
4.8+6.2		S	1.394E−21	8.19	42.89	6.2	32.5	4.99E+33
5.2−2.6		S	1.208E−21	8.39	43.93	8.4	44.0	7.93E+33
5.4−1.2*	Milne 56	C?(P)	4.30E−21	3.39	34.48	4.5	45.8	3.06E+34
5.9+3.1		S	1.24E−21	7.52	43.73	7.5	43.6	8.02E+33
6.1+1.2		F	7.72E−22					
6.4−0.1*	W28	C	2.64E−20	1.18	16.53	2.5	34.9	8.38E+34
6.4+4.0		S	2.04E−22	6.56	59.14	6.5	58.6	2.38E+33
7.0−0.1		S	1.67E−21	9.53	41.61	9.5	41.5	9.75E+33
7.7−3.7	1814-24	S	3.42E−21	5.77	36.92	5.8	37.1	1.60E+34
8.7−5.0		S	9.80E−22	6.01	45.49	5.2	39.3	5.14E+33
8.7−0.1	W30	S?(P)	5.95E−21	2.31	30.24	3.5	45.8	4.24E+34
9.8+0.6		S	4.08E−21	10.11	35.24	12	41.8	2.43E+34
10.0−0.3		?	6.82E−21	12.35	28.61	12	27.8	1.8E+34
11.2−0.3*		C(XP)	2.07E−19	6.28	7.19	5	5.7	2.38E+34
11.4−0.1		S?	1.41E−20	9.20	21.32	9.2	21.3	2.20E+34
12.0−0.1		?	1.08E−20	11.65	23.8	12	24.5	2.18E+34
13.3−1.3		S?	?	?	?	3	46.0	
13.5+0.2		S	2.63E−20	12.82	16.56	13	16.8	2.56E+34
15.1−1.6		S	1.15E−21	5.68	44.29	5.7	44.5	7.72E+33
15.9+0.2		S?	2.15E−20	10.41	17.97	11	19.0	2.62E+34
16.2−2.7		S	1.04E−21	9.11	45.03	8.8	43.5	6.69E+33
16.7+0.1		C	2.82E−20	14.06	16.1	16	18.3	3.32E+34
16.8−1.1		?	4.18E−22	6.72	52.44	6.7	52.3	3.88E+33
17.4−2.3		S	1.25E−21	6.25	43.66	6.3	44.0	8.24E+33
17.8−2.6		S	1.05E−21	6.45	45.01	6.4	44.7	7.08E+33
18.8+0.3	Kes 67	S	2.66E−20	4.14	16.5	8	31.8	9.13E+34
18.9−1.1		C?	5.11E−21	3.35	32.15	3.4	32.6	1.85E+34
20.0−0.2		F	1.51E−20					
21.5−0.9		C	6.27E−19	4.01	4.59	5.5	6.3	7.85E+33
21.8−0.6	Kes 69	S	2.60E−20	2.86	16.65	2.9	16.9	2.51E+34
22.7−0.2		S?	7.35E−21	3.67	27.76	3.7	28.0	1.95E+34
23.3−0.3	W41	S	1.45E−20	2.69	21.11	2.8	22.0	2.37E+34
23.6+0.3		?	1.20E−20	7.81	22.73	8	23.3	2.21E+34
24.7−0.6		S?	5.35E−21	7.23	31.56	9	39.3	2.80E+34
24.7+0.6		C?	6.69E−21	4.68	28.84	5	30.8	2.16E+34
27.4+0.0	4C-04.71	S(AXP)	5.64E−20	10.62	12.16	6.5	7.4	1.10E+34
27.8+0.6		F	3.01E−21			3.2	36.1	1.33E+34
28.6−0.1		S	3.86E−21	11.45	36	11.5	36.1	1.72E+34
28.8+1.5		S?	?	?	?			
29.6+0.1		S(AXP)	9.03E−21	17.43	25.54	11	16.1	7.85E+33
29.7−0.3	Kes 75	C(XP)	1.67E−19	9.26	7.83	6.7	5.7	1.94E+34
30.7−2.0		?	2.94E−22	11.94	55.62	12	55.9	3.11E+33
30.7+1.0		S?	2.09E−21	6.63	40.09	6.6	39.9	1.13E+34
31.5−0.6		S?	9.29E−22	8.77	45.9	8.8	46.1	6.69E+33
31.9+0.0*	3C391	S	1.03E−19	5.52	9.52	8.5	14.7	7.50E+34
32.0−4.9	3C396.1	S?	9.20E−22	2.63	45.98	2.7	47.1	6.93E+33
32.1−0.9		C?	?	?	?			
32.8−0.1	Kes 78	S?	5.73E−21	6.21	30.7	6.3	31.1	1.89E+34
33.2−0.6		S	1.63E−21	7.98	41.8	8	41.9	9.68E+33
33.6+0.1	Kes 79	S	3.31E−20	5.19	15.09	7	20.3	4.66E+34
34.7−0.4*	W44	C(P)	3.66E−20	1.62	14.49	2.8	25.0	7.79E+34

TABLE I *(Continued).*

l,b	Name	Type	Σ	$d_{\Sigma-D}$ (kpc)	$D_{\Sigma-D}$ (pc)	d_{ado} (kpc)	D_{ado} (pc)	L (erg/s)
36.6−0.7		S?	?	?	?			
36.6+2.6	3C396	S	4.77E−22	11.86	51.31	11.6	50.2	4.07E+33
39.2−0.3	HC24	S	5.64E−20	6.04	12.16	7.7	15.5	4.61E+34
39.7−2.0	W50	?	1.78E−21	1.67	41.19	1.7	42.0	1.06E+34
40.5−0.5		S	3.42E−21	5.77	36.92	5.7	36.5	1.55E+34
41.1−0.3		S	2.94E−19	6.38	6.23	6.4	6.2	3.90E+34
42.8+0.6		S	7.84E−22	6.76	47.22	6	41.9	4.67E+33
43.3−0.2*	W49B	S	4.77E−19	5.25	5.13	9	8.8	1.33E+35
43.9+1.6		S?	3.60E−22	3.08	53.78	3.1	54.1	3.57E+33
45.7−0.4		S	1.31E−21	6.77	43.36	6.7	42.9	8.15E+33
46.8−0.3	HC40	S	9.53E−21	5.77	24.98	7.0	30.3	2.97E+34
49.2−0.7	W51	S?	2.68E−20	1.88	16.45	4.0	34.9	1.11E+35
53.6−2.2	3C400.2	S	1.30E−21	4.91	43.38	4.5	39.8	7.00E+33
54.1+0.3		F	3.34E−20			10	4.9	2.16E+33
54.4−0.3*	HC 40	S	2.63E−21	3.31	38.57	3.3	38.4	1.32E+34
55.0+0.3		S	2.51E−22	11.33	57.11	11.3	56.9	2.76E+33
55.7+3.4		S	3.98E−22	7.91	52.87	7	46.8	2.97E+33
57.2+0.8	4C21.53	S?	1.88E−21	11.70	40.8	11.7	40.8	1.07E+34
59.5+0.1		S	1.81E−20	13.17	19.29	11	16.1	1.57E+34
59.8+1.2		?	7.53E−22	9.14	47.54	9.1	47.3	5.73E+33
63.7+1.1		F	4.23E−21					
65.1+0.6		S	2.01E−22	3.04	59.28	3	58.5	2.33E+33
65.3+5.7		S?	1.05E−22	0.83	66.03	0.8	63.5	1.44E+33
65.7+1.2	DA495	?	2.37E−21	7.50	39.26	7.5	39.3	1.24E+34
67.7+1.8		S	2.60E−21	14.83	38.65	14	36.5	1.19E+34
68.6−1.2		?	1.51E−22	8.08	62.2	8	61.6	1.94E+33
69.0+2.7*	CTB 80	?(P)	2.82E−21	1.64	38.13	2	46.5	2.08E+34
69.7+1.0		S	9.41E−22	9.83	45.8	9.5	44.2	6.24E+33
73.9+0.9		S?	2.80E−21	5.96	38.18	5	32	9.72E+33
74.0−8.5*	Cygnus L.	S	8.59E−22	0.83	46.5	0.8	44.6	5.81E+33
74.9+1.2	CTB 87	F	2.82E−20			7.9	15.9	2.43E+34
76.9+1.0		?	2.79E−21	12.61	38.21	12.6	38.2	1.37E+34
78.2+2.1*	DR4	S(D)	1.42E−20	1.22	21.25	1.5	26.2	3.31E+34
82.2+5.3	W63	S	2.92E−21	1.66	37.9	1.7	38.9	1.50E+34
84.2−0.8		S	5.17E−21	6.15	32	5	26	1.19E+34
84.9+0.5		S	3.34E−21	21.05	37.06	10	17.6	3.46E+33
85.4+0.7		S	?	?	?			
85.9−0.6		S	?	?	?			
89.0+4.7*	HB21	S	3.07E−21	1.24	37.6	0.9	27.2	7.70E+33
93.3+6.9*	DA 530	S	2.51E−21	5.75	38.89	3.8	25.7	5.62E+33
93.7−0.2	DA 551	S	1.53E−21	1.82	42.24	1.6	37.2	7.19E+33
94.0+1.0	3C434.1	S	3.01E−21	4.73	37.72	4.7	37.5	1.43E+34
106.3+2.7		?(P)	6.27E−22	4.44	49.01	5.5	60.7	7.85E+33
109.1−1.0*	CTB 109	S(AXP)	3.84E−21	4.43	36.1	5	40.7	2.16E+34
111.7−2.1	Cas A	S(D)	1.64E−17	0.84	1.22	3	4.4	1.06E+36
114.3+0.3*		S(P)	1.82E−22	2.94	60.23	2.8	57.3	2.03E+33
116.5+1.1		S	3.45E−22	2.69	54.16	3.5	70.5	5.82E+33
116.9+0.2*	CTB 1	S	1.17E−21	4.46	44.15	3.5	34.6	4.77E+33
117.7+0.6		(D)				3		
119.5+10.2*	CTA 1	S(D)	6.69E−22	1.85	48.49	1.4	36.7	3.05E+33
120.1+1.4*	Tycho	S	1.32E−19	3.73	8.63	3.3	7.6	2.64E+34
126.2+1.6		S?	2.15E−22	2.88	58.6	2.5	50.9	1.89E+33
127.1+0.5	R5	S	9.66E−22	3.48	45.6	2.5	32.7	3.51E+33
130.7+3.1	SN 1181	F(D)	1.10E−19			3.2	5.8	1.46E+34
132.7+1.3*	HB3	S	1.06E−21	1.93	44.91	2.3	53.5	1.03E+34
156.2+5.7*		S	6.22E−23	2.25	72.08	2.3	73.6	1.14E+33
160.9+2.6	HB9	S	9.85E−22	1.21	45.45	1.2	45.2	6.85E+33
166.0+4.3*	VRO	S	5.47E−22	3.93	50.14	3.8	48.5	4.37E+33
166.2+2.5	OA 184	S	2.63E−22	2.45	56.67	2.5	57.7	2.97E+33
179.0+2.6		S?	2.15E−22	2.88	58.6	2.9	59.0	2.55E+33
180.0−1.7*	S 147	S	3.02E−22	1.06	55.37	1	52.4	2.81E+33

TABLE I *(Continued).*

l,b	Name	Type	Σ	$d_{\Sigma-D}$ (kpc)	$D_{\Sigma-D}$ (pc)	d_{ado} (kpc)	D_{ado} (pc)	L (erg/s)
182.4+4.3		S	7.22E−23	4.83	70.3	3.5	50.9	6.35E+32
184.6−5.8	Crab	F(P)	4.47E−18			2	3.5	1.80E+35
189.1+3.0*	IC 443	C	1.19E−20	1.75	22.84	1.5	19.6	1.56E+34
192.8−1.1	PKS 0607	S	4.95E−22	2.25	50.99	2.3	52.2	4.57E+33
205.5+0.5*	Monoceros	S	4.98E−22	0.80	50.94	1	64.0	6.92E+33
206.9+2.3	PKS 0646	S?	3.76E−22	3.74	53.37	3.4	48.5	3.00E+33
260.4−3.4*	Puppis A	S(D)	6.52E−21	1.83	29.13	2	31.9	2.25E+34
261.9+5.5		S	1.25E−21	4.33	43.66	3.3	33.3	4.71E+33
263.9−3.3*	Vela	C(P)	4.05E−21	0.48	35.33	0.45	33.4	1.53E+34
266.2−1.2		S(D)	5.23E−22	1.45	50.53	1.0	34.9	2.16E+33
272.2−3.2		S?	268E−22	12.94	56.5	9	39.3	1.40E+33
279.0+1.1		S	5.00E−22	1.84	50.9	1.8	49.7	4.20E+33
284.3−1.8	MSH10-53	S(P)	2.87E−21	5.44	38.01	5.2	36.3	1.29E+34
286.5−1.2		S?	1.35E−21	11.85	43.12	10	36.4	6.05E+33
289.7−0.3		S	3.70E−21	7.93	36.64	7.9	36.5	1.67E+34
290.1−0.8		S	2.38E−20	3.64	17.26	5.5	26.1	5.48E+34
291.0−0.1		C	1.23E−20	5.55	22.5	5.5	22.3	2.09E+34
292.0+1.8	MSH11-54	C	2.35E−20	6.09	17.33	5.0	14.3	1.62E+34
292.2−0.5		S(P)	3.51E−21	7.30	36.76	7.5	37.8	1.70E+34
293.8+0.6		C	1.88E−21	7.01	40.8	6.9	40.1	1.03E+34
294.1−0.0		S	>1.88E−22	?	<59.92	4		>1.38E+33
296.1−0.5		S	1.30E−21	4.91	43.39	4.9	43.3	8.30E+33
296.5+10*	PKS1209	S(D)	1.23E−21	1.97	43.77	1.8	40.1	6.72E+33
296.8−0.3	1156−62	S	4.84E−21	6.75	32.88	6.8	33.1	1.80E+34
298.5−0.3		?	3.01E−20	10.71	15.68	11	16.1	2.62E+34
298.6−0.0		S	6.97E−21	9.36	28.36	9.3	28.2	1.87E+34
299.2−2.9		S	3.80E−22	13.00	53.29	12	49.2	3.11E+33
299.6−0.5		S	8.91E−22	12.22	46.22	12.2	46.1	6.43E+33
301.4−1.0		S	3.71E−22	6.30	53.49	6.3	53.5	3.60E+33
302.3+0.7		S	2.60E−21	7.82	38.64	7.8	38.6	1.31E+34
304.6+0.1	Kes 17	S	3.29E−20	6.53	15.13	6.5	15.1	2.56E+34
308.1−0.7		S	1.07E−21	11.86	44.84	11	41.6	6.28E+33
308.8−0.1		C?(P)	3.76E−21	5.11	36.4	8	57.0	4.15E+34
309.2−0.6		S	5.85E−21	7.79	30.44	6	23.5	1.09E+34
309.8+0.0		S	5.39E−21	4.97	31.48	5	31.7	1.84E+34
310.6−0.3	Kes 20B	S	1.18E−20	9.91	22.95	9.9	22.9	2.12E+34
310.8−0.4	Kes 20A	S	6.27E−21	8.49	29.6	8.5	29.6	1.87E+34
311.5−0.3		S	1.81E−20	13.17	19.29	12	17.6	1.87E+34
312.4−0.4		S	4.69E−21	3.01	33.29	3	33.2	1.75E+34
315.4−2.3*	RCW 86	S	4.18E−21	2.86	34.88	2.7	33.0	1.54E+34
315.4−0.3		?	3.86E−21	7.02	36.03	7	35.9	1.69E+34
315.9−0.0		S	3.44E−22	9.96	54.18	10	54.4	3.46E+33
316.3−0.0	MSH14-57	S	7.41E−21	4.72	27.66	4.7	27.5	1.19E+34
317.3−0.2		S	5.85E−21	9.51	30.45	9.5	30.4	1.83E+34
318.2+0.1		S	>4.19E−22	?	<52.42	4		
318.9+0.4		C	1.43E−21	7.16	42.69	7.2	42.9	8.96E+33
320.4−1.2*	RCW 89	C(P)	7.37E−21	2.72	27.72	4.2	42.8	4.58E+34
320.6−1.6		S	?	?	?			
321.9−1.1		S	>6.53E−22	?	<48.69	5		>3.67E+3
321.9−0.3		S	2.74E−21	4.93	38.31	4.9	38.1	1.35E+34
322.5−0.1		C	1.00E−21	10.38	45.31	10.3	45.0	6.88E+33
323.5+0.1		S	2.67E−21	10.17	38.48	10	37.8	1.30E+34
326.3−1.8	MSH15-56	C	1.51E−20	1.88	20.73	2.0	22.1	2.5E+34
327.1−1.1		C	3.25E−21	7.11	37.24	6.5	34.1	1.28E+34
327.4+0.4	Kes 27	S	1.02E−20	3.97	24.27	5.0	30.5	3.24E+34
327.4+1.0		S	1.46E−21	10.46	42.57	10.4	42.3	8.88E+33
327.6+14.6*	SN 1006	S	3.18E−21	4.28	37.38	2	17.5	3.29E+33
328.4+0.2	MSH15-57	F	9.03E−20			17.4	25.5	1.96E+35
329.7+0.4		S	>3.88E−21	?	<35.96	3.3		>1.6E+34
330.0+15.0	Lupus L.	S	1.63E−21	0.80	41.8	0.8	41.9	9.69E+33
330.2+1.0		S?	6.22E−21	9.28	29.7	9.3	29.8	1.87E+34

TABLE I   *(Continued).*

l,b	Name	Type	Σ	$d_{\Sigma-D}$ (kpc)	$D_{\Sigma-D}$ (pc)	d_{ado} (kpc)	D_{ado} (pc)	L (erg/s)
332.0+0.2		S	8.36E−21	7.56	26.34	7.5	26.1	1.95E+34
332.4−0.4*	RCW 103	S	4.21E−20	4.70	13.69	3.7	10.8	1.66E+34
332.4+0.1	Kes 32	S(D)	1.74E−20	4.48	19.58	4	17.5	1.80E+34
335.2+0.1		S	5.46E−21	5.12	31.3	5.1	31.1	1.80E+34
336.7+0.5		S	6.45E−21	8.52	29.26	8.5	29.2	1.87E+34
337.0−0.1	CTB 33	S	1.00E−19	19.73	9.63	11	5.4	7.86E+33
337.2−0.7		S	8.36E−21	14.96	26.34	12	21.1	1.25E+34
337.3+1.0	Kes 40	S	1.34E−20	5.58	21.78	5.6	21.9	2.17E+34
337.8−0.1	Kes 41	S	5.02E−20	5.99	12.75	8	17.1	4.98E+34
338.1+0.4		S	2.68E−21	8.81	38.47	8.8	38.4	1.34E+34
338.3−0.0		S	1.65E−20	8.65	20.03	8.6	19.9	2.24E+34
338.5+0.1		?	2.23E−20	6.79	17.71	6.8	17.7	2.40E+34
340.4+0.4			1.08E−20	9.75	23.8	9.7	23.7	2.03E+34
340.6+0.3		S	2.09E−20	10.33	18.18	10.3	18.1	2.29E+34
341.2+0.9		C(P)	6.41E−22	8.94	48.83	6.8	37.1	3.00E+33
341.9−0.3		S	7.68E−21	13.35	27.27	13.3	27.2	1.91E+34
342.0−0.2		S	4.00E−21	10.82	32.77	10.8	32.7	1.76E+34
342.1+0.9		S	8.36E−22	16.91	46.71	16.9	46.7	6.17E+33
343.0−6.0		S	?	?	?			
343.1−2.3		C?	1.18E−21	4.74	44.13	4.7	43.8	7.64E+33
343.1−0.7		S	2.07E−21	5.80	40.15	5.8	40.2	1.13E+34
344.7−0.1		C?	3.76E−21	12.51	36.4	12.5	36.4	1.69E+34
345.7−0.2		S	2.51E−21	22.09	38.89	18	31.7	8.40E+33
346.6−0.2		S	1.88E−20	8.19	18.97	8.2	19.0	2.33E+34
347.3−0.5		S?	?	?	?	6.0		
348.5−0.0		S?	1.51E−20	7.14	20.77	7.1	20.7	2.18E+34
348.5+0.1	CTB 37A	S	4.82E−20	2.97	12.97	6.0	26.2	1.12E+35
348.7+0.3	CTB 37B	S	1.35E−20	4.38	21.67	7.0	34.5	5.52E+34
349.2−0.1		S	3.90E−21	16.85	35.87	16	34.1	1.55E+34
349.7+0.2		S	6.02E−19	6.75	4.66	12.0	8.2	1.24E+35
350.0−2.0		S	1.93E−21	3.10	40.62	3.1	40.6	1.08E+34
351.2+0.1		C?	1.54E−20	10.08	20.6	10.1	20.6	2.20E+34
351.7+0.8		S	5.97E−21	6.54	30.19	6.5	30.0	1.83E+34
351.9−0.9		S	2.51E−21	12.83	38.89	12.8	38.8	1.27E+34
352.7−0.1		S	1.25E−20	11.10	22.36	11	22.1	2.09E+34
353.9−2.0		S	8.91E−22	12.22	46.22	12	45.4	6.23E+33
354.1+0.1		C?	?	?	?			
354.8−0.8		S	1.17E−21	8.00	44.18	8	44.2	7.75E+33
355.6−0.0		S	9.41E−21	12.48	25.12	12	24.2	1.87E+34
355.9−2.5		S	7.12E−21	7.43	28.11	7.4	28.0	1.89E+34
356.2+4.5		S	9.63E−22	6.27	45.62	6	43.6	6.23E+33
356.3−0.3		S	5.86E−21	11.88	30.41	11.8	30.2	1.81E+34
356.3−1.5		S	1.51E−21	8.40	42.35	8.4	42.3	9.15E+33
357.7−0.1	MSH 17-39	?	2.32E−19	4.82	6.86	7.0	9.9	7.85E+34
357.7+0.3		S	2.61E−21	5.53	38.62	5.5	38.4	1.31E+34
358.0+3.8		S	1.56E−22	5.59	61.8	5.2	57.5	1.75E+33
359.0−0.9		S	6.54E−21	4.35	29.09	4.4	29.4	1.92E+34
359.1−0.5		S	3.66E−21	5.23	36.51	5.2	36.3	1.64E+34
359.1+0.9		S	5.70E−21	9.19	30.76	9.2	30.8	1.83E+34

2.2   Abbreviations for Data of Point Sources Genetically Connected with SNRs

1. Types of point sources:
    (a) Radio pulsar: PSR
    (b) X-ray pulsar: XRP
    (c) X-ray point source: XPS
    (d) Neutron star: NS

2. Distance of point source from the geometrical center of SNR: $\beta = \Delta\theta/\theta$ ($\Delta\theta$: angular distance of point source from the geometrical center of SNR; θ: average value of angular size of SNR)
3. Characteristic age of pulsar: τ (kyr)
4. Dispersion measure: DM pc cm^{-3}

Values of F_1, θ and α for SNRs were taken from Green (2001). Adopted distance values which were used in constructing the Σ–D diagram are also given below.

2.3 Calibrator Supernova Remnants

SNR G4.5+6.8

$d = 4.8 \pm 1.4$ kpc [1], 5 kpc [2], 4.5 ± 1 kpc [3], 4.1 ± 0.9 kpc [4], $d = 4.4$ kpc from the historical date and $d = 4.8 - 6.4$ kpc from HI line measurements [5], $d = 4.8$ kpc adopted.

Kepler is about 500 pc above the galactic plane that it must be in a very low-density medium. So, its surface brightness must be much less than the surface brightness value corresponding to its diameter and its distance must be much less than the distance value found from the Σ–D relation.

[1] Reynoso and Goss, 1999; [2] Borkowski *et al.*, 1992; [3] Bandiera, 1987; [4] Braun, 1987; [5] Green, 2001.

SNR G6.4−0.1

$d = 3.5$–4 kpc [1, 20], $d = 2.5$ kpc [2], $d = 2.5$ kpc adopted.

In the direction of this SNR, at 1.6 kpc, there is SGR OB1 association. Interstellar absorption, A_V, and N_{HI} values of the stars, which are members of this association ($1 = 5°.97$–$7°.16$, $b = -0°.48$–$+0°.62$), are $\sim 1^m$ and $\sim 2 \times 10^{21}$ cm^{-2}, respectively [3].

$N_{HI} = (7$–$11) \times 10^{21}$ cm^{-2}, $N_{HI} = 3.5 \times 10^{21}$ cm^{-2} [4], $N_{HI} = 4.7 \times 10^{21}$ cm^{-2} [5, 6]; E(B-V) $= 1$–1.3^m [4].

Since the SNR has $A_V = 3$–4^m and $N_{HI} > 3.5 \times 10^{21}$ cm^{-2} its distance is assumed to be considerably larger than the OB association's distance.

MS [10, 13, 16, 17]; MC $n = 10^5$ cm^{-3} [9, 10], $n = 2.5 \times 10^4$ cm^{-3} [11, 12], $n = 2.5 \times 10^4$ cm^{-3} [13, 15, 16], $n = 30$ cm^{-3} (the average value in the shell) [14], $n_0 = 0.1$ cm^{-3} [4], $n_0 = 0.23$ cm^{-3} (the average value in front of the SNR) [6].

$E = 10^{51}$ erg [4], $E = 4 \times 10^{50}$ erg [6]; $F_x = 6.2 \times 10^{-11}$ erg cm^{-2} s (0.5–2.4 keV) [6]; $t = 2.5 \times 10^3$ yr [4], $t = (1$–$2.5) \times 10^4$ yr [6], $t = (3.5$–$15) \times 10^4$ yr [7, 8], $t = 6 \times 10^4$ yr [14]; $M_x = (19$–$26)$ M$_\odot$ [4]; $B = 0.2$ mG (in the shell) [18].

If the SNR's explosion energy is 10^{51} erg, the swept-up matter's mass must be about $\leq 2 \times 10^4$ M$_\odot$. In order to sweep-up such a mass the average density of the medium must be $n_0 \leq 5$ cm^{-3}. The SNR is in a very high-density medium [9, 10].

The SNR interacts with the molecular cloud in the east of the SNR and this interaction has increased its radio and X-ray luminosity. There are many maser and H II regions in the field. The relativistic particles have energy of 2×10^{47} erg. It is C-type also in the X-ray band. The SNR is expanding in a very thick medium [19].

Since the medium is very dense, the values of the magnetic field and the explosion energy as well as the temperature and the X-ray luminosity must be large that this SNR should be very high above the Σ–D line.

[1] Green, 2001; [2] Sahibov, 1983; [3] Aydin *et al.*, 1997; [4] Long *et al.*, 1991; [5] Rho and Petre, 1998; [6] Rho *et al.*, 1996; [7] Kaspi *et al.*, 1993; [8] Rowell *et al.*, 2000; [9] Claussen *et al.*, 1997; [10] Claussen *et al.*, 1999a; [11] Wooten, 1981; [12] Denoyer, 1983; [13] Frail *et al.*, 1994a; [14] Marsden *et al.*, 1999; [15] Denoyer, 1979a,b; [16] Frail *et al.*, 1996; [17]

Reach and Rho, 1998; [18] Koralesky *et al.*, 1998a; [19] Dubner *et al.*, 2000; [20] Ankay and Guseinov, 1998.

SNR G31.9+0.0

$d = 8.5$ kpc (from 21 cm H I line) [1], $d = 7.2$ kpc [2], $d = 7.2$ kpc (from 21 cm H I line) [3, 4], $d = 9$ kpc [3, 4], $d = 8.5$ kpc adopted.

$N_{HI} = 2.4 \times 10^{22}$ cm^{-2} (0.1–2.4 keV) [3, 4].

The SNR is expanding in a dense medium [2]; MC [2]; $n_0 \sim 5$–10 cm^{-3} (the average value in front of the SNR) [4], $n \sim 2 \times 10^5$ cm^{-3} (the average value behind the SNR, *i.e.* for the cloud) [5]; $M_{\text{total}} \cong 700$ M$_\odot$ [4].

[1] Green, 2001; [2] Frail *et al.*, 1996; [3] Radhakrishnan *et al.*, 1972; [4] Rho and Petre, 1996; [5] Reach and Rho, 1998.

SNR G34.7−0.4

$d = 2.6$ kpc [2], $d = 2.5$ kpc [3], $d = 2.5$ kpc (from 21 cm H I line) [4], $d = 2.8$ kpc adopted.

$N_{HI} = (1.6$–2.1$) \times 10^{22}$ cm^{-2} [3].

No H$_2$O maser source [9]; MC [1, 7, 8]; $n_0 = 6$ cm^{-3} (the average value in front of the SNR) [3], $n_0 = 1$ cm^{-3} [3].

$E \cong 10^{51}$ erg [3]; $M = 10^3$ M$_\odot$ [3]; $B = 0.2$ mG [10].

Point Source PSR J1856+0113

$d = 2.8$ kpc [5, 11], $d = 3.3$ kpc [6]; $\tau = 2.03 \times 10^4$ yr [11]; $\beta = 0.51$ [13], $\beta = 0.6$ [14].

A pulsar wind nebula (PWN) was found around this pulsar and this PWN is positionally coincident with the EGRET source [12].

[1] Giaconi *et al.*, 1997; [2] Braun *et al.*, 1989; [3] Cox *et al.*, 1999; [4] Green, 2001; [5] Kaspi, 2000; [6] Taylor *et al.*, 1996; [7] Frail *et al.*, 1996; [8] Denoyer, 1979a,b; [9] Claussen *et al.*, 1999; [10] Koralesky *et al.*, 1998a; [11] Guseinov *et al.*, 2002; [12] Roberts *et al.*, 2001; [13] Lorimer *et al.*, 1998; [14] Allakhverdiev *et al.*, 1997.

SNR G54.4−0.3

$d = 3.3$ kpc [1], $d = 3.3$ kpc adopted.

MC and OB-associations are present [1]; $n = 30$ cm^{-3} for MC [1]; $M_s \cong 5 \times 10^4$ M$_\odot$ [1].

[1] Junkes *et al.*, 1992.

SNR G74.0−8.5

$d = 0.8$ kpc [1], $d = 0.7$ kpc [2], $d = 1.4$ kpc [4], $d = 460$ pc [5], $d = 1.3 \pm 0.7$ kpc (kinematic distance) [3], $d = 440^{+130}_{-100}$ pc (using the shock wave's velocity and proper motion) [6], $d = 0.8$ kpc adopted.

E(B-V) $= 0.08^m$ [3] (As the absorption in this direction is small [7], this value is in accordance with a distance value of about 0.8–1 kpc).

There is no open cluster in the direction of this SNR. In this direction, between 0.8–1.5 kpc, the reddening is almost constant [7].

[1] Minkowski, 1958; [2] Braun *et al.*, 1989; [3] Greidanus and Strom, 1992; [4] Sakhibov and Smirnov, 1983; [5] Braun and Strom, 1986; [6] Blair *et al.*, 1999; [7] Neckel and Klare, 1980.

SNR G78.2+2.1

$d = 1.2$ kpc [1], $d = 1.5$ kpc [2–6], $d = 1.5$ kpc adopted.

MC [2]; $n_0 \geq 4$ cm^{-3} [2].

The SNR is probably expanding inside a cavity [7].

$E_k = 1.7 \times 10^{49}$ erg (for the shell) if $d = 1.5$ kpc [2]; $M_x = 10^2$ M$_\odot$ [7].

In the direction of the SNR ($1 = 76°.8$, $b = 1°.44$), at $d = 1.37$ kpc, there is Cygnus OB-association in which there are many massive stars [8].

Point Source RX J2020.2+4026 [9]

[1] Braun *et al.*, 1989; [2] Landecker *et al.*, 1980; [3] Green, 1989; [4] Huang and Thaddeus, 1985; [5] Brazier *et al.*, 1996; [6] Lorimer *et al.*, 1998; [7] Lozinskaya *et al.*, 2000; [8] Melnik and Efremov, 1995; [9] Brazier and Johnston, 1999.

SNR G109.1−1.0

$d = 4$ kpc [1], $d = 3.6$ kpc [2], $d = 5$ kpc [5, 12], $d = 5.6$ kpc [9], $d = 6$ kpc [13], $d = 5$ kpc adopted (since, the SNR is in a very dense medium and its explosion energy is high).

$E(\text{B-V}) = (0.79–1.2)^m$ [3]; $N_{HI} = (8–10) \times 10^{21}$ cm^{-2} [4], $N_{HI} = 4 \times 10^{21}$ cm^{-2} [5].

$kT = 0.17–0.56$ keV [7]; $F_x = 7.8 \times 10^{-11}$ erg cm^{-2} s (0.2–2.4 keV) [7]; $L_x = 3.2 \times 10^{37}$ erg/s [7].

MC [6, 8]; $n = 20$ cm^{-3} (for the clouds) [3, 11], $n_0 = 0.25$ cm^{-3} (the average value in front of the SNR) [5]. $E = 10^{51}–10^{52}$ erg [5].

Point Source AXP 1E 2259+586

$d = 5.6$ kpc [9]; $N_{HI} = 9 \times 10^{21}$ cm^{-2} [7], $N_{HI} = 9.3 \times 10^{22}$ cm^{-2} (0.5–20 keV) [10].

[1] Green, 1989; [2] Braun *et al.*, 1989; [3] Fesen and Hurford, 1995; [4] Rho and Petre, 1993; [5] Morini *et al.*, 1988; [6] Parmar *et al.*, 1998; [7] Rho and Petre, 1997; [8] Tatematsu *et al.*, 1990; [9] Hughes *et al.*, 1984; [10] Patel *et al.*, 2001; [11] Gotthelf and Vasisht, 1998; [12] Gaensler, 2000, [13] Hulleman *et al.*, 2000.

SNR G114.3+0.3

$d = 3.0–3.8$ kpc [1], $d = 2.5–3$ kpc [2, 3], $d = 2.8$ kpc adopted.

$n_0 = 0.1$ cm^{-3} (the average value for the medium) [4].

The SNR's shell expanded inside a H II region and has reached to the boundary of the H II region [4].

This SNR together with the SNRs G116.5+1.1 and G116.9+0.2 (CTB 1) are inside a supercavity [4].

In the direction of the SNR ($l = 115°.5$, $b = 0°.25$), at $d = 2.3$ kpc, there is Cas 5 OB association [5].

Point Source PSR J2337+6151 [6]

$d = 2.5$ kpc (from 21 cm HI line) [7], $d = 2.5$ kpc [6], $d = 2.8$ kpc [8]; $\tau = 4.07 \times 10^4$ yr [8, 11]; $\beta = 0.08$ [9, 10].

[1] Green, 2001; [2] Reich and Braunsfurth, 1981; [3] Fesen *et al.*, 1997; [4] Fich, 1986; [5] Melnik and Efremov, 1995; [6] Lyne *et al.*, 1996; [7] Becker *et al.*, 1996; [8] Guseinov *et al.*, 2002; [9] Lorimer *et al.*, 1998; [10] Furst *et al.*, 1993; [11] Taylor *et al.*, 1996.

SNR G116.9+0.2

$d = 3.1$ kpc [1], $d = 2.3$ kpc [2], $d = 2.8–4$ kpc [3], $d = 3.5$ kpc adopted.

$N_{HI} = 7 \times 10^{21}$ cm^{-2} [5]; $A_V = 2.2–3.2$ [6].

In the direction of this SNR, at 2.5 kpc, there is an O6-type star (HD/BD 108). For this star $N_{HI} = 3 \times 10^{21}$ cm^{-2} [4] that the SNR's distance must be larger than the distance of this star.

In this direction, there is no star formation region beyond 3 kpc. If the distance of this SNR is ∼2.7 kpc, then it may be in the star formation region which include CAS OB2 and CAS OB5 associations. There is also a young open cluster (C2355+609, $t = 4 \times 10^7$ yr) at about 3.7 kpc in this direction [8].

For the stars in this direction, located at 1–4 kpc, $A_V \sim 2^m$ and does not reach a value of 3^m [7].

The SNR is expanding in a low-density supercavity which also include G114.3+0.3 and G116.5+1.1. The shock wave front does not have a regular but a discontinuous shape [6].

[1] Hailey and Craig, 1994; [2] Braun *et al.*, 1989; [3] Green, 2001; [4] Diplas and Savage, 1994; [5] Craig *et al.*, 1997; [6] Fesen *et al.*, 1997; [7] Neckel and Klare, 1980; [8] Lynga, 1987.

SNR G119.5+10.2

$d = 1.4$ kpc [1–5], $d = 1.4$ kpc adopted.

$N_{HI} = 2.8 \times 10^{21}$ cm^{-2} [3], $N_{HI} = (1.1–2.5) \times 10^{21}$ cm^{-2} [2], $N_{HI} = 3.8 \times 10^{21}$ cm^{-2} [7]; $A_V = 1.3$ [5].

MC [7]; $n \sim 1$ cm^{-3} (for the clouds in front of the SNR) [5], $n_0 \sim 0.03$ cm^{-3} (the average value in front of the SNR) [5], $n_0 \sim 0.02$ cm^{-3} (the average value in front of the SNR) [2].

$E = 3 \times 10^{49}$ erg [2]; $M_s = 13\,\mathrm{M}_\odot$ [2]; $B = 2.9 \times 10^{-6}$ G [2].

OIII emission line ($\lambda = 5010\,\text{Å}$, $\Delta\lambda = 28\,\text{Å}$) is very strong as in SNRs G65.3+5.7 and G126.2+1.6 [8].

Point Source RX J0007.0+7302 [6]

[1] Pineault *et al.*, 1993; [2] Seward *et al.*, 1995; [3] Slane *et al.*, 1997; [4] Brazier *et al.*, 1998; [5] Mavromatakis *et al.*, 2000; [6] Brazier and Johnston, 1999; [7] Rho and Petre, 1998; [8] Fesen *et al.*, 1981.

SNR G120.1+1.4

$d = 2.2\,\mathrm{kpc}$ [1], $d = 2.3\,\mathrm{kpc}$ (from shock wave velocity model), $d = 4$–$5\,\mathrm{kpc}$ (from 21 cm HI line) [2], $d = 4.6\,\mathrm{kpc}$ [3], $d = 3\,\mathrm{kpc}$ (from X-ray observations of Ginga satellite) [4], $d = 3.3\,\mathrm{kpc}$ adopted.

$A_V = 2.1 \pm 0.5$ [5].

In the direction of this SNR, there are Cas OB4 (at 2.7 kpc; $l = 118°$–$121°.5$, $b = -2°.7$–$+2°.3$) and Cas OB7 (at 1.8 kpc; $l = 121°.8$–$124°.2$, $b = -0°.5$–$+2°.7$) associations [8]. If the distance of this SNR is less than 3 kpc, *i.e.* if it is located close to the OB associations, its diameter must be less than 6 pc. Then, how can it be possible that the surface brightness of this young S-type SNR located in a dense medium is much less than the surface brightness value corresponding to its diameter? On the other hand, if Tycho's distance is close to 4 kpc, then the SNR may be in a low-density medium that its surface brightness can be such a low value [6, 7].

[1] Albinson, 1986; [2] Green, 2001; [3] Schwarz *et al.*, 1995; [4] Fink *et al.*, 1994; [5] Chevalier *et al.*, 1980; [6] Reynoso *et al.*, 1999; [7] Reynoso *et al.*, 1997; [8] Garmany and Stencel, 1992.

SNR G132.7+1.3

$d = 2.2 \pm 0.2\,\mathrm{kpc}$ (from 21 cm H I line) [1], $d = 2.2\,\mathrm{kpc}$ [2], $d = 2.7\,\mathrm{kpc}$ [3], $d = 2.2\,\mathrm{kpc}$ (from optical data) [4], $d = 2.3\,\mathrm{kpc}$ adopted.

The SNR's center is bright in X-ray [5].

$N_{HI} \sim 3 \times 10^{21}\,\mathrm{cm}^{-2}$ [5], $N_{HI} = 6.9 \times 10^{21}\,\mathrm{cm}^{-2}$ [6]; $N_{HI} = 4.3 \times 10^{21}\,\mathrm{cm}^{-2}$ [10]; E(B-V) = 0.71 [7].

The SNR interacts with the gas in the star formation region [1]. There are H II regions around the SNR [4]. HB3 is expanding in a dense medium [5].

$kT = 0.33\,\mathrm{keV}$ [10]; $E = 3.1 \times 10^{50}$ erg [6].

Point Source PSR J0215+6218

$d = 2.3\,\mathrm{kpc}$ [8], $d = 3.2\,\mathrm{kpc}$ [9]; $\tau = 1.3 \times 10^7$ yr [9].

[1] Routledge *et al.*, 1991; [2] Green, 2001; [3] Braun *et al.*, 1989; [4] Gray *et al.*, 1999; [5] Rho *et al.*, 1998; [6] Galas *et al.*, 1980; [7] Fesen *et al.*, 1995a; [8] Lorimer *et al.*, 1998; [9] Guseinov *et al.*, 2002; [10] Rho and Petre, 1998.

SNR G166.0+4.3

$d = 4.5\,\mathrm{kpc}$ [2], $d = 3\,\mathrm{kpc}$ [3, 4], $d = 3.8\,\mathrm{kpc}$ adopted.

The SNR's center is bright in X-ray [6–8].

In this direction, there is no identified star formation region at this distance, but the outer arm (Persei) of the galaxy is passing through. There is AUR OB2 association in the direction $l = 172°$–$174°$, $b = -1°.8$–$+2°.0$ at 3.2 kpc. The distance of the SNR from the galactic plane at 4.5 kpc is 340 pc. Because of these the SNR is expected to be in a low-density medium.

$N_{HI} = 2.9 \times 10^{21}\,\mathrm{cm}^{-2}$ [5].

The SNR is expanding in a low-density cavity [8].

[1] Landecker *et al.*, 1989; [2] Green, 2001; [3] Allakhverdiev *et al.*, 1986b; [4] Braun *et al.*, 1989; [5] Guo and Burrows, 1997; [6] Pineault *et al.*, 1987; [7] Rho *et al.*, 1994; [8] Fesen *et al.*, 1997.

SNR G180.0−1.7

$d = 0.8$ kpc [1], $d = 1$ kpc (by identifying some indications of the SNR in the spectrums of the stars in front of and behind the SNR) [2], $d = 1$ kpc adopted (since distances of stars are used to find the distance of the SNR, this value is much more reliable).

[1] Braun *et al.*, 1989; [2] Phillips *et al.*, 1981.

SNR G189.1+3.0

$d = 1.5$ kpc [1–3], $d = 1.5$–2 kpc (from the interaction of the SNR with the MC [10], $d = 1.5$ kpc adopted.

$N_{HI} = (1–3) \times 10^{21}$ cm^{-2} [3].

MC [5, 6]; $n = 10$–20 cm^{-3} (the average value in front of the SNR) [8].

In the north-eastern part $V \cong 100$ km/s and the density in front is $n = 10$–1000 cm^{-3}, whereas in the southern part $V \cong 30$ km/s and the density in front is $n = 10^4$ cm^{-3} [8].

Not an H_2O maser source [7].

In the near infrared region the SNR's luminosity is 1.3×10^{36} erg/s [8].

In the direction of the SNR ($l = 188°.9$, $b = 3°.44$), at $d = 1.34$–1.65 kpc, there is Gem OB1 association in which there are 16 massive stars [11, 12]. $B = 500\,\mu$G [4].

Point Source CXOU J061705.3+222127 [9]

In this region there is a point X-ray source [4]; $N_{HI} = 1.3 \times 10^{21}$ cm^{-2} [4, 9].

The radio flux at 327 MHz of the X-ray point source is not greater than 2 mJy [9].

[1] Fesen, 1984; [2] Allakhverdiev *et al.*, 1986b; [3] Asoaka and Aschenbach, 1994; [4] Keohane *et al.*, 1997; [5] Denoyer, 1979a,b; [6] Frail *et al.*, 1996; [7] Claussen *et al.*, 1999; [8] Rho *et al.*, 2001; [9] Olbert *et al.*, 2001; [10] Green, 2001; [11] Melnik and Efremov, 1995; [12] Blaha and Humphreys, 1989.

SNR G260.4−3.4

$d = 1.5$ kpc [1], $d = 2$ kpc [2], $d = 2.2 \pm 0.3$ kpc (from 21 cm HI line) [3, 4], $d = 1.9$–2.5 kpc [5], $d = 1.3^{+0.6}_{-0.8}$ kpc [6], $d = 2$ kpc adopted.

$N_{HI} = (2–6) \times 10^{21}$ cm^{-2} [7], $N_{HI} = (2.9–4.7) \times 10^{21}$ cm^{-2} [5, 8], $N_{HI} = 1.4 \times 10^{21}$ cm^{-2} [9].

There is a B0.7 Ib type star (HD 69882; $l = 259°.5$, $b = -3°.9$, $d = 2.1$ kpc) in the same region of Puppis A and for this star $N_{HI} = 1.6 \times 10^{21}$ cm^{-2} [10].

Puppis A is in the direction of Vela X and, like the star formation regions in this part of the galaxy, it is below the geometrical plane of the galaxy.

Puppis A is not exactly in the direction of the star formation regions. Distances of the OB associations in the star formation region do not exceed 1.5–1.8 kpc [11, 12].

On the other hand, it is seen from the distribution of neutral hydrogen (H I) in the galaxy that the cold clouds in the direction of Puppis A are in general nearer than 1.5–1.8 kpc [1].

Diameter of this SNR has reached to 32 pc and it has gone out of the H II region it was in. Eastern part of the remnant is interacting with the H I cloud [3].

There are OH clouds in front of the SNR, but no sign of an interaction between the SNR and the clouds has been found [6].

$n_0 \cong 0.4$–0.5 cm^{-3} (the average value in front of the SNR) [3], $n = 100$ cm^{-3} (for X-ray emitting region) [1], $n = 10$–1000 cm^{-3} (for clouds) [3], $n_0 = 3$ cm^{-3} (the average value in front of the SNR) [7], $n_0 = 1$ cm^{-3} [9].

N, O and Ne are abundant in the SNR [2].

Point Source RX J0822−4300 [13]

$N_{HI} = (4–8) \times 10^{21}$ cm^{-2} [2].

The region $< 30''$ around the pulsar in the SNR has been examined. The upper limit of the radio luminosity of a possible pulsar-powered nebula is 3 orders of magnitude less than what would be expected if RX J0822−4300 was an energetic young radio pulsar beaming away

from us. RX J0822−4300 has some properties which are very different compared to most of the young pulsars' properties [14].

[1] Braun *et al.*, 1989; [2] Petre *et al.*, 1996; [3] Reynoso *et al.*, 1995; [4] Green, 2001; [5] Zavlin *et al.*, 1999; [6] Woermann *et al.*, 2000; [7] Winkler *et al.*, 1981a,b; [8] Blair *et al.*, 1995; [9] Berthiaume *et al.*, 1994; [10] Diplas and Savage, 1994; [11] Melnik and Efremov, 1995; [12] Humphreys, 1978; [13] Pavlov *et al.*, 1999; [14] Gaensler *et al.*, 2000b.

SNR G263.9−3.3

Recent distance estimates of Vela are as follows: $d = 0.25$ kpc [1], $d = 0.25 \pm 0.03$ kpc [2], $d \sim 0.28$ kpc [3], $d = 0.25, 0.3$ kpc [14].

The stars which are in front of, behind, and interacting with Vela have been identified [4]. The distance of Vela is given as 250 ± 30 pc in [4].

In estimating the distance one should also consider that Vela SNR expands in a dense environment. Its magnetic field is $B \sim 6 \times 10^{-5}$ G [5] and its explosion energy is $(1-2) \times 10^{51}$ erg [4]. These values have large errors, but the values themselves are also large. If we take all of these values into account, then, in the Σ–D diagram, it is not accceptable to put Vela at the same position with SNR G327.6+14.6 (remnant of type Ia supernova explosion at 500 pc above the galactic plane [6]) which expands in a low-density medium.

In the direction of Vela remnant, none of the young open clusters nor OB associations have distances as small as 0.25 kpc [7–9]. Among the open clusters in the direction of Vela SNR (none of them has a distance value as small as 0.25 kpc) Pismis 4 ($l = 262°.7, b = -2°.4$) and Pismis 6 ($l = 264°.8, b = -2°.9$), which have the most precise distance values and are exactly in the direction of Vela SNR, are located at 0.6 kpc and 1.6 kpc, respectively [1]. Since progenitors of SNRs (and pulsars) are massive stars one would expect Vela to be closer to the star formation region instead of a distance value of 0.25 kpc.

If the distance value of 0.45 kpc (which is close to the previous distance estimation of 0.5 kpc [10]) is adopted for Vela PSR, then the average electron density along the line of sight will be $n_e = 0.153$ cm^{-3}. The pulsar with the second largest n_e value (~ 0.113 cm^{-3}) is for PSR J1302−6350 ($l = 304°.2, b = -0°.9, d = 1.3$ kpc, with a Be type companion, variable wind in the environment) and the third largest n_e value (0.107 cm^{-3}) belongs to PSR J1644−4569 ($l = 339°.2, b = -0°.2$). Since the flux of PSR J1644−4569 at 1400 MHz is larger than any other known pulsars' flux value at the same frequency, we can estimate its distance as not more than 4.5 kpc. Average value of n_e for the rest of pulsars is about 0.04 cm^{-3} [13]. So, it is not possible to accept a distance value of 0.25 kpc for Vela pulsar and Vela SNR. All we could do is to reduce our initial distance estimate of 0.45 kpc to at most 0.4 kpc.

$V = 170$ km/s [11]; $kT = 0.086$–0.17 keV [12]; $A_V = 0.56$ [11]; $E = (1-2) \times 10^{51}$ erg [4]; $B \sim 6 \times 10^{-5}$ G [5].

From the above discussion $d = 0.45$ kpc adopted.

Point Source PSR J0835−4510

DM = 68.2 cm^{-3} pc; $d = 0.5$ kpc [15]; $\tau = 1.1 \times 10^4$ yr [13, 15]; $\beta = 0.29$ [16], $\beta = 0.3$ [17].

[1] Ögelman *et al.*, 1989; [2] Cha *et al.*, 1999; [3] Bocchino *et al.*, 1999; [4] Danks, 2000; [5] de Jager *et al.*, 1996; [6] Hamilton *et al.*, 1997; [7] Efremov, 1989; [8] Berdnikov and Efremov, 1993; [9] Aydin *et al.*, 1997; [10] Green, 2000; [11] Raymond *et al.*, 1997; [12] Kahn *et al.*, 1985; [13] Guseinov *et al.*, 2002; [14] Green, 2001; [15] Taylor *et al.*, 1996; [16] Lorimer *et al.*, 1998; [17] Allakhverdiev *et al.*, 1997.

SNR G296.5+10.0

$d = 1.5$ kpc [1–3], $d = 1$–2 kpc [4], $d = 2.1$ kpc [5], $d = 1.8$ kpc adopted.

$N_{HI} = 1.4 \times 10^{21}$ cm^{-2} ($d = 1$–2 kpc) [6], $N_{HI} = (1.1-1.6) \times 10^{21}$ cm^{-2} ($d = 1$–2 kpc) [5], $N_{HI} = 4 \times 10^{20}$ cm^{-2} (0.1–10 keV) [7], $N_{HI} = 4 \times 10^{20}$ cm^{-2} [2]; $A_V(r) = 0.5^m (d = 1$–2 kpc) [8].

$n_0 = 0.2 \, \text{cm}^{-3}$ (the average value in front of the SNR) [7]; $E = 2 \times 10^{50} \, \text{erg}$ [7], $E = 6 \times 10^{50} \, \text{erg}$ ($d = 1$–$2 \, \text{kpc}$) [4], $E > 2 \times 10^{49} \, \text{erg}$ [5].

Mass of the neutral hydrogen in the SNR is more than $1900 \, \text{M}_\odot$ ($d = 1$–$2 \, \text{kpc}$) [5].

Point Source 1E 1207.4−5209 [2, 5]

There is a hole in the HI clouds, at exactly the center of the SNR and the neutron star is located at this position that it is genetically connected with the SNR [5].

[1] Kaspi *et al.*, 1996; [2] Mereghetti *et al.*, 1996; [3] Zavlin *et al.*, 2000; [4] Roger *et al.*, 1988; [5] Giacani *et al.*, 2000; [6] Kellett *et al.*, 1987; [7] Vasisht *et al.*, 1997; [8] Ruiz, 1983.

SNR G315.4−2.3

$d = 2.8 \, \text{kpc}$ [1, 2], $d = 2.5 \, \text{kpc}$ [3, 4], $d = 2.8 \, \text{kpc}$ (kinematic) [6], $d = 2.5 \, \text{kpc}$ [10], $d = 2.5 \, \text{kpc}$ (the SNR is located in an OB-association) [13], $d = 2.7 \, \text{kpc}$ adopted.

$N_{HI} = (1$–$4) \times 10^{21} \, \text{cm}^{-2}$ [2, 5], $N_{HI} = 3 \times 10^{21} \, \text{cm}^{-2}$ [10].

$n_0 = 0.2 \, \text{cm}^{-3}$ (the average value in front of the SNR), $n = 10 \, \text{cm}^{-3}$ (for the clouds) [6], $n = 0.2 \, \text{cm}^3$ (the average value in front of the SNR) [12], $n_0 = 0.3 \, \text{cm}^{-3}$ (the average value in front of the SNR) [13]; $E = 6.6 \times 10^{50} \, \text{erg}$ [6].

The part of the remnant, which is bright in radio, is also bright in X-ray [7]. X-ray synchrotron radiation has been observed [7–9].

The abundances of O, Ne, Mg, and Si are more than the abundance of Fe that the SNR was formed due to a type-II supernova [10].

The SNR's morphology looks like the morphology of Tycho. The SNR has expanded inside a cavity and now it seems that it is expanding in the boundary of the cavity. This leads to a rapid drop in SNR's expansion velocity [11].

In the direction of the SNR ($l = 315°.5$, $b = -2°.75$), at $d = 2.5 \, \text{kpc}$, there is Cir OB1 association [14].

[1] Greidanus and Strom, 1992; [2] Petruk, 1999; [3] Braun *et al.*, 1989; [4] Green, 2001; [5] Nugent *et al.*, 1984; [6] Rosado *et al.*, 1996; [7] Borkowsky, 2001; [8] Allen *et al.*, 1998; [9] Asvarov *et al.*, 1990; [10] Bamba *et al.*, 2000; [11] Dickel *et al.*, 2001; [12] Long and Blair, 1990; [13] Borkowsky *et al.*, 2001; [14] Blaha and Humphreys, 1989.

SNR G320.4−1.2

$d = 3.6 \, \text{kpc}$ [1], $d = 4 \, \text{kpc}$ [2], $d = 5.2 \, \text{kpc}$ (from 21 cm HI line) [3], $d = 5.2 \, \text{kpc}$ [4], $d = 4 \, \text{kpc}$ [11], $d = 4.2 \, \text{kpc}$ adopted.

$N_{HI} = 9 \times 10^{21} \, \text{cm}^{-2}$ [5], $N_{HI} = 9.5 \times 10^{21} \, \text{cm}^{-2}$ [6], $N_{HI} = 6 \times 10^{21} \, \text{cm}^{-2}$ [7].

$n = 100 \, \text{cm}^{-3}$ (in the X-ray emitted part) [1]; $E = (1$–$2) \times 10^{51} \, \text{erg}$ [4]; $M = 28 \, \text{M}_\odot$ (possible) [10]; $B \sim 8 \times 10^{-6} \, \text{G}$ (in the plerionic part) [10].

Point Source PSR J1513−5908 [8, 9]

$d = 4.2 \, \text{kpc}$ [9, 12]; $N_{HI} = 5.9 \times 10^{21} \, \text{cm}^{-2}$ [11]; $\tau = 1.55 \times 10^3 \, \text{yr}$ [9, 12]; $\beta = 0.24$ [13]; a jet has been observed [11].

[1] Braun *et al.*, 1989; [2] Allakhverdiev *et al.*, 1986b; [3] Green, 2001; [4] Gaensler *et al.*, 1999a; [5] Seward *et al.*, 1984; [6] Greiveldinger *et al.*, 1995; [7] Trussoni *et al.*, 1996; [8] Allakhverdiev *et al.*, 1997; [9] Taylor *et al.*, 1996; [10] du Plessis *et al.*, 1995; [11] Tamura *et al.*, 1996; [12] Guseinov *et al.*, 2002; [13] Lorimer *et al.*, 1998.

SNR G327.6+14.6

$d = 0.7 \pm 0.1 \, \text{kpc}$ (from Sedov's model) [1], $d = 1.5$–$2.5 \, \text{kpc}$ [8], $d = 1.7$–$3.1 \, \text{kpc}$ [4], $d = 2 \, \text{kpc}$ [7], $d = 1.8 \pm 0.3 \, \text{kpc}$ [2–4], $d = 2 \, \text{kpc}$ adopted.

$N_{HI} = (3.9$–$5.7) \times 10^{20} \, \text{cm}^{-2}$ [1], $N_{HI} = 1.8 \times 10^{21} \, \text{cm}^{-2}$ [9]; $A_V = 0.31$ [10].

$n_0 = 0.4 \, \text{cm}^{-3}$ (ambient density) [1], $n_0 = 0.1 \, \text{cm}^{-3}$ (in front of the SNR) [12], $n_0 \sim 0.02 \, \text{cm}^{-3}$ [11].

$E > 4.4 \times 10^{49} \, \text{erg}$ [1], $E = 10^{51} \, \text{erg}$ [12].

$B = (6$–$10) \times 10^{-6} \, \text{G}$ [9], $B = (3$–$6) \times 10^{-6} \, \text{G}$ [12].

Using the age ($t \sim 1000$ yr) and the expansion velocity (16,600 km/s) of this SNR its diameter is found to be ~ 17 pc. As the angular diameter of SN 1006 is $30'$ the lower limit for its distance value should be 1.9 kpc [5–7].

[1] Willingale *et al.*, 1996; [2] Long *et al.*, 1988; [3] Roger *et al.*, 1988; [4] Green, 2001; [5] Fesen, 1988; [6] Wu *et al.*, 1993; [7] Winkler and Long, 1997; [8] Schaefer, 1996; [9] Koyama *et al.*, 1995; [10] Laming *et al.*, 1996; [11] Krishner *et al.*, 1987; [12] Reynolds, 1996.

SNR G332.4−0.4

$d = 4$ kpc [9], $d = 3.7$ kpc adopted.

$A_V = 4.5^m$ [1]. This value is comparable with the average A_V value of 6.3^m [3] for the stars at $d = 3.4$ kpc [2] in this direction. The distance has mostly been assumed to be 3.3 kpc [4–7].

In the direction of RCW 103, there is R103 cluster located at 4 kpc [8].

MC [15]; $n = 1000$ cm^{-3} (for the clouds) [8], $n \geq 1000$ cm^{-3} (for the MC) [14]. Density of the gas clouds behind the shock wave is relatively low ($n_e \sim 10^3$ cm^{-3}) [11].

The SNR's angular radius has increased $1''.8 \pm 0''.2$ in 25 years [13].

$N_{HI} = 6.8 \times 10^{21}$ cm^{-2} [10] value shows the possibility that RCW 103 might be related with the cluster R103. If the SNR is in the same region with the cluster, then it is possible that the remnant is expanding in a dense medium.

The SNR has an approximately spherical shape. It is bright and has a thick shell. Northern part of the shell interacts with the molecular cloud. The SNR can be assumed to have formed due to a supernova explosion 1000 years ago [12].

[1] Oliva *et al.*, 1990; [2] Caswell *et al.*, 1975; [3] Neckel and Klare, 1980; [4] Tuohy and Garmire, 1980; [5] Gotthelf *et al.*, 1997; [6] Kaspi *et al.*, 1996; [7] Green, 2001; [8] Braun *et al.*, 1989; [9] Allakhverdiev *et al.*, 1986b; [10] Gotthelf *et al.*, 1999b; [11] Oliva *et al.*, 1999; [12] Dickel *et al.*, 1996; [13] Carter *et al.*, 1997; [14] Meaburn and Allan, 1986; [15] Frail *et al.*, 1996.

SNR G5.4−1.2

$d = 4.5$ kpc (from 21 cm HI line) [1], $d \cong 5$ kpc [2], $d > 4.3$ kpc (from 21 cm HI line) [3], $d = 4.5$ kpc adopted.

$n_0 > 3 \times 10^{-3}$ cm^{-3} (in front of the SNR) [4].

PSR J1801−2451

SNR–PSR J1801−2451 connection [1, 4]; $d = 4.5$ kpc [6], $d = 4.4$ kpc [5]; $\tau = 1.5 \times 10^4$ yr [5, 6]; $\beta = 0.8$ [7]; $\beta \sim 1$ [8].

[1] Frail *et al.*, 1994b; [2] Caswell *et al.*, 1987; [3] Green, 2001; [4] Frail and Kulkarni, 1991; [5] Taylor *et al.*, 1996; [6] Guseinov *et al.*, 2002; [7] Allakhverdiev *et al.*, 1997; [8] Lorimer *et al.*, 1998.

SNR G11.2−0.3

$d = 5$ kpc (from 21 cm HI line) [1], $d = 5$ kpc adopted.

$N_{HI} \cong 10^{22}$ cm^{-2} [3], $N_{HI} = 1.38 \times 10^{22}$ cm^{-2} [4]; $E \sim 10^{48}$–2.4×10^{19} erg [2]; $t \sim 2$ kyr [7].

Point Source AX J1811−1926

$d = 5$ kpc [5]; $\tau = 2.4 \times 10^4$ yr [6].

If the pulsar's real age is 2.4×10^4 yr and if the SNR is a historical one, then the two age values contradict with each other. The possibility of a genetic connection between the radio-quiet pulsar and the SNR is examined in [7].

[1] Green, 2001; [2] Bandiera *et al.*, 1996; [3] Reynolds *et al.*, 1994; [4] Vasisht *et al.*, 1996; [5] Kaspi, 2000; [6] Torii *et al.*, 1999; [7] Roberts *et al.*, 2000.

SNR G43.3−0.2

$d = 8.5$ kpc [1], $d = 12.5$–14 kpc (from 21 cm HI line) [2], $d = 9$ kpc adopted.

$N_{HI} = 4 \times 10^{22}$ cm^{-2} (0.5–10 keV) [3].

The medium around the SNR seems to be highly dense from X-ray observations [4].

[1] Braun *et al.*, 1989; [2] Green, 2001; [3] Fujimoto *et al.*, 1995; [4] Hwang *et al.*, 1999.

SNR G69.0+2.7

$d = 1.3$ kpc [1], $d = 2$ kpc adopted; $E = 10^{51}$ erg.

Point Source J1952+3252 (*radio and X-ray pulsar*) *[4]*

$d = 2.5$ kpc [2–4], $d = 2$ kpc [5]; $N_{HI} = 3 \times 10^{21}$ cm^{-2} [2, 3]; $\tau = 1.07 \times 10^5$ yr [4, 5]; $\beta = 0.14$ [6], $\beta = 0.15$ [7].

[1] Braun *et al.*, 1989; [2] Safi-Harb *et al.*, 1995; [3] Ögelman and Buccheri, 1987; [4] Taylor *et al.*, 1996; [5] Guseinov *et al.*, 2002; [6] Lorimer *et al.*, 1998; [7] Allakhverdiev *et al.*, 1997.

SNR G89.0+4.7

$d = 0.8$ kpc (from the connection of the remnant with the association Cyg OB7) [1, 2], $d = 0.9$ kpc adopted.

[1] Huang and Thaddeus 1985; [2] Tatematsu *et al.*, 1990.

SNR G93.3+6.9

$d = 3.8$ kpc [1], $d = 2.5$ kpc (from 21 cm HI line) [2], $d = 3.8$ kpc adopted ($z = 420$ pc, $D = 26$ pc).

$N_{HI} = 5.7 \times 10^{21}$ cm^{-2} [2]; $E = 3.9 \times 10^{50}$ erg [1].

The type-Ia supernova has exploded 5000 years ago [1].

As this SNR is in a very low-density medium, its position on the Σ–D diagram should be well below the Σ–D line.

[1] Landecker *et al.*, l999; [2] Green, 2001.

SNR G156.2+5.7

The data from ROSAT X-ray satellite were examined using Sedov model. Taking the results found from this model and $N_{HI} = 8.8 \times 10^{20}$ cm^{-2} value into account $d = 3$ kpc [1, 3]. $d = 1.3$ kpc [4]; $D = 100$ pc if $d = 3$ kpc [4].

$N_{HI} = 9 \times 10^{20}$ cm^{-2} [2, 3].

There is no star formation region in the direction of this SNR, but there is an open cluster for which the distance is not known. Both of the distance values correspond to $z > 100$ pc (for $d = 1.3$ kpc, $z = 130$ pc). The facts that there is no star formation region in this direction and that $z > 130$ pc show that the remnant is in a low-density medium. So, the SNR's diameter (and distance) is not expected to be larger than the diameter value corresponding to its surface brightness in the Σ–D diagram. The diameter might be less than the diameter corresponding to its surface brightness. As a result, $d = 2$ kpc adopted ($z = 200$ pc).

[1] Pfeffermann *et al.*, 1991; [2] Yamauchi *et al.*, 1993; [3] Reich *et al.*, 1992; [4] Yamauchi *et al.*, 1999.

SNR G205.5+0.5

$d = 0.8$ kpc (from optical data), $d = 1.6$ kpc (from radio data) [1], $d = 1.6$ kpc [2], $d = 1$ kpc adopted.

[1] Green, 2001; [2] Odegard, 1986.

SNR G111.7−2.1

$d = 2.8$ kpc [1], $d = 3.4$ kpc (by examining the SNR's dynamics) [2].

Cas A has no projection on the OB-associations and none of these OB-associations, which are in the directions close to the SNR, has a distance >3 kpc [3, 4].

$N_{HI} = 1.2 \times 10^{21}$ cm^{-2} [5]; $E \sim 10^{51}$ erg [6, 10].

$M_s + M_{Ej} = 7$–$12\,M_\odot$ [5], $M_{Ej} \sim 4\,M_\odot$, $M_s + M_{Ej} \sim 12\,M_\odot$ [6].

Since Cas A was born because of a massive star's explosion in a dense interstellar medium, its distance was adopted as 3 kpc. This SNR was not used as a calibrator.

Point Source RQNS CXO J2323+5848 [7]

$d = 3.4$ kpc [9]; $N_{HI} = 1.1 \times 10^{22}$ cm^{-2} [8]; $A_V = 5^m$ [9].

[1] Green, 2001; [2] Reed *et al.*, 1995; [3] Humphreys, 1978; [4] Garmany and Stencel, 1992; [5] Favata *et al.*, 1997; [6] Vink *et al.*, 1998; [7] Brazier and Johnston, 1999; [8] Chakrabarty *et al.*, 2001; [9] Kaplan *et al.*, 2001; [10] Wright *et al.*, 1999.

SNR G130.7+3.1

$d = 3.2$ kpc [1–5], $d = 2.2$ kpc [6], $d = 2.6$ kpc [7], $d = 3$ kpc adopted.

The SNR is plerion in x-ray.

$N_{HI} = 1.8 \times 10^{21}$ cm^{-2} (2–10 keV) [1, 8], $N_{HI} = 2 \times 10^{21}$ cm^{-2} (0.5–4.5 keV) [9], $N_{HI} = (3\text{–}4) \times 10^{21}$ cm^{-2} [10], $N_{HI} = 3 \times 10^{21}$ cm^{-2} [3].

$A_V = 1.3 \pm 0.2$ (if this value is correct, then, according to [11] $d < 1$ kpc); $B = 3 \times 10^{-3}$ G [10].

X and radio PSR J0205+6449 [12, 13]

$d = 3.2$ kpc [14]; $\tau = 5.5 \times 10^3$ yr [14].

[1] Roberts *et al.*, 1993; [2] Frail and Moffett, 1993; [3] Helfand *et al.*, 1995; [4] Lorimer *et al.*, 1998; [5] Green, 2001; [6] Braun *et al.*, 1989; [7] Allakhverdiev *et al.*, 1986b; [8] Davelaar *et al.*, 1986; [9] Becker *et al.*, 1982; [10] Torji *et al.*, 2000; [11] Neckel and Klare, 1980; [12] Murray *et al.*, 2002; [13] Camilo *et al.*, 2002; [14] Guseinov *et al.*, 2002.

SNR G184.6−5.8

$d = 2$ kpc [1], $d = 2$ kpc adopted.

$N_{HI} = 3 \times 10^{21}$ cm^{-2} [3]; E(B-V) $= 0.52^m$ [3]; $R = 3.1^m$ [3].

$E \sim 10^{49}$ erg; $L_x = 10^{37}$ erg/s (2–10 keV) [5], $L_x = 2.5 \times 10^{37}$ erg/s [6].

$\Sigma < 4.3 \times 10^{22}$ W m^{-2} Hz^{-1} ster^{-1} (if the SNR has a shell) [2].

The CIV ion's line at $\lambda = 1550$ Å shows that there may be a shell near Crab moving with a velocity of 2500 km/s. $E = 1.5 \times 10^{49}$ erg [3].

Point Source J0534+2200

$d = 2$ kpc; $\beta \sim 0.1$ [4]; $\tau = 1.26 \times 10^3$ yr [7, 8].

[1] Green, 2001; [2] Frail *et al.*, 1995; [3] Sollerman *et al.*, 2000; [4] Lorimer *et al.*, 1998; [5] Davelaar *et al.*, 1986; [6] Becker *et al.*, 1982; [7] Taylor *et al.*, 1996; [8] Guseinov *et al.*, 2002.

After examining the data of these SNRs and the point sources in them, we adopted distance values for the SNRs.

Among the 34 SNRs given above the first 23 ones have the most reliable distance values. For the next 8 SNRs the distance values are relatively less reliable. The last 3 SNRs presented above (Cas A (G111.7−2.1), Crab (G184.6−5.8), and SN 1181 (G130.7+3.1)) were not chosen as calibrators; the surface brightness value of Cas A is extraordinarily high and, Crab and SN 1181 are F-type SNRs. These SNRs are shown on the Σ–D diagram, because their distances are known precisely and their diameters are small. We included them in the Σ–D diagram just to see their positions on the diagram.

3 CONSTRUCTING Σ–D RELATION USING CALIBRATORS

Using the 31 SNRs given above (for which reliable distance values were determined) we constructed the Σ–D relation (Fig. 1). In the Σ–D diagram, F-type historical SNRs Crab and SN 1181, for which the distances are well known, are shown as cross ($\times$) signs. As mentioned above, for F-type SNRs Σ–D relation can not be used, though the positions of Crab and SN 1181 are shown on the Σ–D diagram just to see deviations of their positions from the Σ–D relation.

SNR Cas A has the highest energy among the Galactic SNRs which were formed by SN explosion in the last two thousand years (for all of these SNRs dates of explosion

are known). The massive shell of Cas A is expanding through a dense medium, so that, the magnetic field behind the shock wave is more intense and the situation is more convenient in order to accelerate the electrons (independent of the acceleration mechanism). Because of these reasons Cas A, for which the distance is well known, deviates from the Σ–D line more than the other SNRs ($\Sigma < 10^{-18}\,\mathrm{W\,m^{-2}\,Hz^{-1}\,ster^{-1}}$) do. In our galaxy, this SNR has the highest Σ (and also luminosity) value and it's very high Σ value makes it unique.

As seen from Figure 1, the historical SNRs G4.5+6.8 (Kepler), G332.4−0.4 (RCW 103) and G327.6+14.6 (SN 1006) are located below the Σ–D line. Since, Kepler and SN 1006 are very far away from the Galactic plane they are expanding in a low-density medium and because of this they have surface brightness values much less than the surface brightness values corresponding to their diameters. SNRs G43.3−0.2 (W49B), G6.4−0.1 (W28), G320.4−1.2 (RCW89) and G132.7−1.3 (HB3) are located above the Σ–D line.

For the calibrator SNRs shown in Figure 1 two Σ–D relations with different slopes were constructed; one for the SNRs having $\Sigma \le 3.7 \times 10^{-21}\,\mathrm{W\,m^{-2}\,Hz^{-1}\,sr^{-1}}$ ($D \ge 36.5\,\mathrm{pc}$) and the other for the SNRs with $\Sigma > 3.7 \times 10^{-21}\,\mathrm{W\,m^{-2}\,Hz^{-1}\,sr^{-1}}$ ($D < 36.5\,\mathrm{pc}$):

$$\Sigma = 8.4^{+19.5}_{-6.3} \times 10^{-12} D^{-5.99^{+0.38}_{-0.33}}\,\mathrm{W\,m^{-2}\,Hz^{-1}\,sr^{-1}} \tag{4}$$

and

$$\Sigma = 2.7^{+2.1}_{-1.4} \times 10^{-17} D^{-2.47^{+0.20}_{-0.16}}\,\mathrm{W\,m^{-2}\,Hz^{-1}\,sr^{-1}} \tag{5}$$

Since we have used the flux values at 1 GHz given in Green (2001) these equations are valid only for 1 GHz frequency.

In Figure 2, the relation between radio luminosity (at 1 GHz) and diameter values of the calibrator SNRs shown in Figure 1 are given. Similar to the Σ–D relation, we found 2 equations for L–D relation with an intersection at $L = 5300\,\mathrm{Jy\,kpc^2}$, $D = 36.5\,\mathrm{pc}$; one for the SNRs having $L > 5300\,\mathrm{Jy\,kpc^2}$, $D < 36.5\,\mathrm{pc}$ and the other for the SNRs having $L \le 5300\,\mathrm{Jy\,kpc^2}$, $D \ge 36.5\,\mathrm{pc}$:

$$L = 2.45 \times 10^4 D^{-0.43}\,\mathrm{Jy\,kpc^2} \tag{6}$$

and

$$L = 5.38 \times 10^9 D^{-3.84}\,\mathrm{Jy\,kpc^2} \tag{7}$$

These dependences are not as reliable as the Σ–D dependences given above [Eqs. (4) and (5)] that we did not give their errors which are very large. Similar to the Σ–D diagram, in Figure 2 Cas A and Crab have very high radio luminosities. Considering the other calibrator SNRs (except SNRs G156.2+5.7 and G114.3+0.3 which have reliable distance and radio luminosity values) we see that the luminosity decreases only a bit with respect to the diameter (see Fig. 2). Does radio luminosity of SNRs actually change only a little bit until their diameters reach to values 40–50 pc?

If, during the evolution of SNRs, $L(F)$ value does not really change much then the slope of the Σ–D relation must be −2 (*i.e.* $\Sigma \sim D^{-2}$), but no one has claimed that such an equation for SNRs is valid, yet. In this work, such an equation is not valid for all the calibrator SNRs, either.
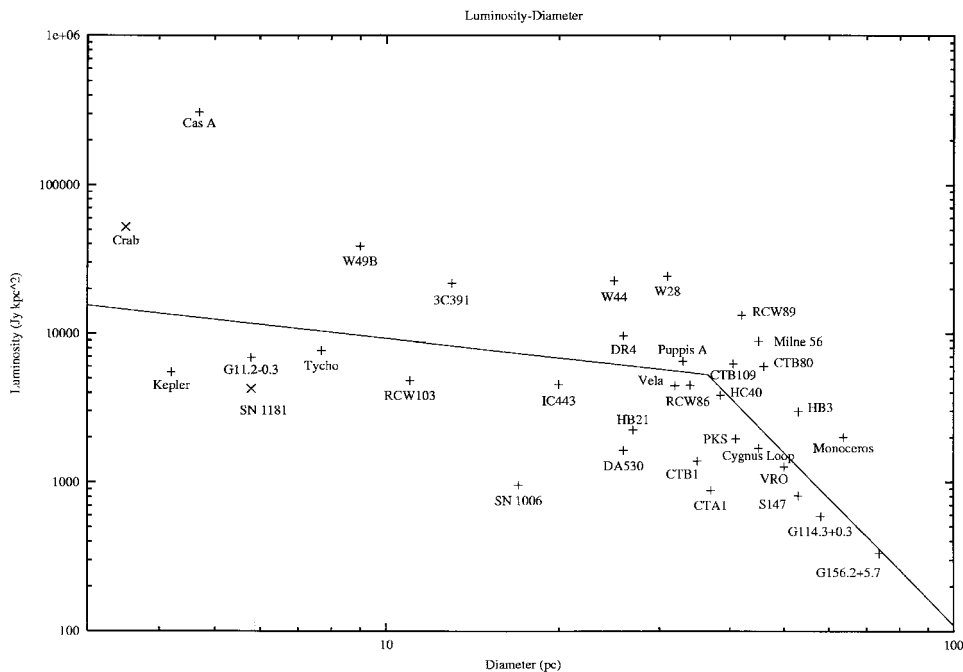
FIGURE 2   Luminosity (Jy kpc^2) versus diameter (pc) diagram (see text).

The most contribution for the luminosity seen to be almost constant is mainly due to the SNRs W44 (G34.7−0.4), W28 (G6.4−0.1) and RCW 89 (G320.4−1.2) which are high-density medium. As it is known that, the ejected mass of Type I SN is less than the ejected mass of Type II SN, but expansion velocity of Type I SNe's remnants is greater, about 15,000 km/s on average. If such a remnant expands in a very low-density medium (as often is the case), then in a very short time it can reach to a large diameter of about SNR SN1006's diameter. For such a case, dense ultra-relativistic particles and high magnetic fields can not be expected. So that, such SNRs have low luminosity and surface brightness values corresponding to their diameters in the *L–D* and Σ–*D* diagrams.

This is also true for SNR G4.5+6.8 (Kepler, SN1604) which is in the galactic center direction and 570 pc above the galactic plane. As Kepler's age and diameter are 400 yr and 4 pc, respectively, its radio luminosity being 5.5 times higher than SN1006's radio luminosity is normal (see Fig. 2). This shows that for S-type SNRs expanding through low-density medium the luminosity decreases considerably, about 5 times, even only in 1000 years.

As seen in Figure 1, the S-type SNR G93.3+6.9 (DA530, $z = 420$ pc), which is the third most distant SNR from the galactic plane (after Kepler and SN 1006), also is well below the Σ–*D* line. This Ia type SN is assumed to have been formed 5000 years ago. Its explosion energy is 3.9×10^{50} erg. Its diameter is 26 pc (Landecker *et al.*, 1999). Since this SNR is in a very low-density medium, it has a low luminosity (see Fig. 2). It must be noted that, errors in age and explosion energy values of SNRs are not small, because these values are found using some not-so-precise observational data and theoretical models.

The other S-type SNRs with respect to their distances from the galactic plane are, respectively: G166.0+4.3 (VRO 42.05.01, $z = 277$), G296.5+10 (PKS1209-51/52, $z = 261$), and G119.5+10.2 (CTA 1, $z = 248$ pc). Among these, G166.0+4.3 is located in the outer (Persei) arm of the Galaxy. There is a sharp increase in reddening values of the stars located

between 3–4 kpc in the direction of this SNR (Neckel and Klare, 1980) that the density of dust in this region should be high. So, this SNR can not be assumed to expand in a low-density medium. On the other hand, since SNRs G296.5+10 and G119.5+10.2 are absolutely out of star formation regions, they can be assumed to be in lower density medium. Because of this, their surface brightness and luminosity values are low as expected (see Figs. 1 and 2).

As seen in Table I and Figures 1 and 2, SNR G156.2+5.7 has the lowest surface brightness and radio luminosity values among the calibrator SNRs. We can say that Kepler and SN 1006-like SNRs will have such low surface brightness and radio luminosity values when their diameters reach to about 60–70 pc.

In Σ–D and L–D diagrams, SNRs G156.2 + 5.7, Kepler and SN1006 are roughly on the same lines that these lines can be assumed to be the evolutionary tracks of S-type SNRs which evolve in very low-density medium. The equations of these tracks are (D in pc):

$$\Sigma = 5 \times 10^{-17} D^{-3.32} \, \mathrm{W \, m^{-2} \, Hz^{-1} \, ster^{-1}} \tag{8}$$

$$L = 3 \times 10^4 D^{-1.16} \, \mathrm{Jy \, pc^2} \tag{9}$$

From the definitions $\Sigma \sim F/\theta^2$ and $L \sim Fd^2$, the relation between Σ and L is:

$$\Sigma \sim L/D^2 \tag{10}$$

Using the Σ–D Eqs. (4) and (5) for the SNRs having diameters greater than and less than 36.5 pc, and Eq. (10) we can find 2 equations; one for the SNRs having smaller diameters:

$$L \sim D^{-0.47} \tag{11}$$

and the other one for the SNRs having larger diameters:

$$L \sim D^{-4} \tag{12}$$

If we compare these 2 equations with Eqs. (6) and (7), respectively, we see that the values of powers are very close to each other. Therefore, Eqs. (6) and (7) can be considered to be correct, in principle.

4 THEORETICAL BASIS

As known from synchrotron radiation theory, radiation (in radio band) per unit volume at a certain frequency (spectral density) is given as (Ginzburg, 1981)

$$j_v = 1.35 \times 10^{-27} b(\alpha)(6.26 \times 10^4)^\alpha K_e B_{-5}^{\alpha+1} v_{\mathrm{GHz}}^{-\alpha} \, \mathrm{erg \, cm^{-3} \, s^{-1} \, ster^{-1} \, Hz^{-1}} \tag{13}$$

Here, $b(\alpha)$ is a function of α, B is the magnetic field of the region which emits in units of 10^{-5} Gauss, v_{GHz} is frequency of radiation in units of GHz, K_e is the coefficient in the energy spectrum (distribution) of ultrarelativistic electrons.

$$N_e \mathrm{d}E = K_e E^{-\gamma} \mathrm{d}E \, \mathrm{electron/cm^3} \tag{14}$$

Here, $\gamma = 2\alpha + 1$. In the shells of S- and C-type SNRs electrons are accelerated mainly by regular (Bell–Krymsky) mechanism (Bell, 1978a; 1978b; Krymsky, 1977). In order to apply this mechanism to SNRs, it is necessary to choose acceptable values for the Bell coefficients (Allakhverdiev *et al.*, 1986d), but here we consider the acceleration under strong shock propagation, in general. This mechanism gives the number and energy distribution of electrons, which are accelerated in the strong shock wave, in units of density of the medium and velocity of the shock wave. K_e, given in Eq. (14), depends on volume density of unaccelerated electrons in the shock wave (n) and velocity of the shock wave (V):

$$K_e \sim nV^{2\alpha} \tag{15}$$

If we apply the regular mechanism to the acceleration in the SNR's shock wave we get:

$$j_v = 9.69 \times 10^{-30} b(\alpha)(3.41 \times 10^{-9})^{\alpha} \Phi_e \alpha n V_8^{2\alpha} B_{-5}^{\alpha+1} v_{\mathrm{GHz}}^{-\alpha} \, \mathrm{erg\, cm^{-3}\, s^{-1}\, ster^{-1}\, Hz^{-1}} \tag{16}$$

Here, V_8 is the shock wave velocity in units of 10^8 cm/s and Φ_e is the constant given by Bell.

As seen from Eq. (16), the radiation of the SNR shell's unit volume at a certain frequency (j_v) is related to n, V, and B for radio radiation with spectral index, $\alpha = 0.5$ (note that the spectral indices of S and C-type SNRs are always close to 0.5 and this confirms the Bell mechanism):

$$j_v \sim nVB^{1.5} \tag{17}$$

Using the observational data of SNRs in X-ray, optical, and radio bands Tagieva (2002) showed that

$$n \sim D^{-0.9\pm0.4}, \quad V \sim D^{-1.3\pm0.3}, \quad B \sim D^{-0.8} \tag{18}$$

Since the magnetic field values are known (with large errors) only of a few of the SNRs, it is not yet possible to find a relation between B and D directly from observations. If the dynamo mechanism to increase the magnetic field is not working, then, as magnetic field is freezed to gas, $B \sim n^{2/3} \sim D^{-0.6}$. If the dynamo is also working a bit, we can roughly assume that $B \sim D^{-0.8}$ as in Eq. (18). Using the relations of Eq. (18) in Eq. (17):

$$j_v \sim D^{-3.4} \tag{19}$$

Shock wave front expands like a shell that its volume increases roughly with D^2. Because of this, luminosity is:

$$L_v \sim D^2 j_v \tag{20}$$

From Eqs. (19) and (20)

$$L \sim D^{-1.4} \tag{21}$$

This is roughly in agreement with the average power of the L–D equations [Eqs. (6) and (7)] found from the L–D diagram (Fig. 2). But using this single equation, instead of using the 2 L–D equations, leads to results with larger errors for some of the SNRs.

As known from observations, while SNR's diameter is increasing most of the parts of the shock wave front do not interact with interstellar clouds, so that, behind the wave from some large low-density regions form. In these regions, as the value of magnetic field intensity is smaller, high-energy ultrarelativistic electrons can hardly be trapped. The electrons in denser regions of the wave front move along the magnetic field lines, which are very disordered, and, after reaching the low-density regions, they can also leave the SNR. It must be noted that, for SNRs with $D \sim 40$ pc the magnetic field, on average, is (2–6) µG (Seward et $al.$, 1995; du Plessis et $al.$, 1995; for G93.7−0.3$B = 2.3$ µG, Uyamker et $al.$, 2001). The lifetime of ultrarelativistic electrons is:

$$t(\mathrm{yr}) = \frac{3 \times 10^2}{H^2(\mathrm{Gauss})E(\mathrm{eV})} \tag{22}$$

Energy and lifetime of the ultrarelativistic electrons, which radiate in such magnetic fields at 1 GHz, are not less than $\sim 5 \times 10^3$ MeV and 4×10^4 yr; the lifetime of ultrarelativistic electrons is comparable to the average lifetime of SNRs that, not only the new-accelerated electrons but mainly the electrons which have already been accelerated do produce the radiation of SNRs. As these electrons leave the low-magnetic field regions of the SNR, the SNR's radiation decreases rapidly. So that, in most of the cases, the part of the shell, which is farther away from the Galactic plane (where the number density of clouds is low), is less bright (Caswell and Lerche, 1979; Allakhverdiev et $al.$, 1983b). Since such a decrease in the radiation is more effective in large-diameter SNRs, the slope of the Σ–D equation for such SNRs should be larger.

5   DISCUSSION AND CONCLUSIONS

In this work, we have constructed the Σ–D relation for C and S-type SNRs. We have also adopted distance and diameter values for all of the Galactic SNRs given in the Galactic SNRs catalog of Green (2001) and also for some recently found SNRs. Although the SNR nature of Sgr A East (G0.0+0.0) and G10.0−0.3 is uncertain, we have included them in Table I, because they are given in the Galactic SNRs catalog (Green, 2001).

As mentioned in the introduction, in the last 45 years many Σ–D relations were constructed and presented in the literature. In some of these works a single linear dependence between log Σ and log D values of calibrator SNRs was given. In other works 2 linear dependences (with 2 different slopes) were given. The most recent Σ–D dependence was given by Case and Bhattacharya (1998): $\Sigma(1\,\mathrm{GHz}) = 2.07^{+3.10}_{-1.24} \times 10^{-17}D^{-2.38\pm0.26}$ W m^{-2} Hz^{-1} ster^{-1} (Cas A is not included).

As seen above, in Case and Bhattacharya (1998) the relation between Σ and D is given with only one equation, instead of two, for the whole set of calibrators. The reason of this is that, for some of the calibrator SNRs having small surface brightness values ($\Sigma < 10^{-21}$ W m^{-2} Hz^{-1} ster^{-1}), they assume diameter (distance) values larger than the values which we have adopted to construct our Σ–D relation (which includes 2 equations with 2 different slopes). So, for small-Σ calibrator SNRs the adopted diameters (distances) given in Case and Bhattacharya (1998) are larger than the diameters (distances) which we have adopted. It is necessary to compare and discuss the SNRs for which the differences in the adopted distance values are the largest. For example, for SNRs G156.2+5.7, G166.0+4.3, G180.0−1.7, and G205.5+0.5 the distances adopted by Case and Bhattacharya (1998) and by us (given in brackets) are, respectively: 3.0 (2.0) kpc,

4.5 (3.8) kpc, 1.5 (1.0) kpc, and 1.6 (1.0) kpc. In Section 2.3, we discussed the distance values of these calibrator SNRs in detail.

There are 3 SNRs which were considered as calibrators by Case and Bhattacharya (1998), but excluded by us in constructing the Σ–D dependence: G116.5+1.1, G160.9+2.6, and G166.2+2.5. The adopted diameter values of these SNRs given in Case and Bhattacharya (1998) differ significantly from our adopted diameter values (Tab. I). The distance values of these SNRs according to Case and Bhattacharya (1998) and the distance values of the SNRs adopted by us (given in brackets) are, respectively: 5 (3.5) kpc, 3.0 (1.2) kpc, and 4.5 (2.7) kpc. We will discuss the distance values of these 3 SNRs below.

For SNR G116.5+1.1 $d = 3.6$–5.2 kpc (Green, 2001) and $d = 4.4$ kpc (Reich and Braunsfurth, 1981; Lorimer *et al.*, 1998) values were given. In the direction of this SNR, there is Persei arm of the Galaxy about 3–4 kpc distant from the Sun. On the other hand, there is no star formation region at ~5 kpc in this direction. In this part of the interstellar medium which is not dense (Fesen *et al.*, 1997), this SNR might reach a diameter of about 70–90 pc at $d = 3.5$–4.4 kpc.

The supercavity in which SNR G116.5+1.1 is located also include G114.3+0.3 and G116.9+0.2 (Fich, 1986). The diameter (distance) of SNR G116.5+1.1 is not expected to be larger than the diameter (distance) of SNR G114.3+0.3, because the surface brightness of SNR G116.5+1.1 is greater than the surface brightness of SNR G114.3+0.3. Also, a few SNRs being located in the same region requires them to be in the Galactic arm. From our Σ–D relation the distance of this SNR is found to be 2.7 kpc. Taking this and the distance values given above into account we have adopted $d = 3.5$ kpc for SNR G116.5+1.1.

For SNR G160.9+2.6 $d = 1.7$ kpc (Braun *et al.*, 1989) and $d < 4$ kpc (Green, 2001) were given. From the Σ–D relation $d = 1.2$ kpc and this value is adopted as the distance of SNR G160.9+2.6. In this direction, between $d = 1$–3 kpc, the interstellar absorption is almost constant (Neckel and Klare, 1980). This shows that the medium ($d = 1$–3 kpc) has a very low density. In this part of the Galaxy there is no star formation region. So, even for small diameter values, the surface brightness of this SNR must be small.

For SNR G166.2+2.5 $d = 8$ kpc (Routledge *et al.*, 1986; Green, 2001), $d = 4.5$ kpc (Landecker *et al.*, 1989), and $d = 2$ kpc (Braun *et al.*, 1989) were given. Since, there is no star formation region at these distances in this direction, this SNR can not be much above the Σ–D line. A distance of 2.5 kpc is found from the Σ–D relation and this value is adopted as the distance of this SNR.

Above, we discussed the escape of relativistic electrons from large-diameter SNRs. Because of this effect, the SNR's luminosity, and also its surface brightness, should decrease rapidly with respect to the diameter of the SNR. So, the Σ–D dependence of large-diameter SNRs should be sharper (with a larger slope) compared to the Σ–D dependence of the SNRs which have smaller diameters.

There is also another such effect; at the initial stages of the evolution, SNRs expand within the HII regions which were created by the progenitors of the SNRs. During this time, as the shock wave has a high velocity its temperature is also high that the X-ray radiation will be high. Expansion velocity of the SNR must decrease a lot when the SNR's shock wave reaches the HII region's boundary and interacts with a dense neutral gas and molecular clouds (Lozinskaya, 1981; Chevalier, 1999; Eikenberry, 2002). But at the same time, the rate of drop of the X-ray radiation should decrease as the mass and density of the gas in the shock wave increases. Naturally, a SNR which has a high explosion energy and which is expanding through a dense medium must have a higher X-ray luminosity compared to a SNR with a lower explosion energy expanding through a lower-density medium. It is seen that, after the SNR reaches the boundary of the HII region, which was formed by the progeni-tor O-type star, a small increase in the SNR's size will be accompanied by a sharp decrease in

the SNR's radio and X-ray luminosity. Depending on sizes of the HII regions, surface brightness of SNRs will begin to drop sharply at different values of the diameter. We have assumed a value of $D = 36.5$ pc as the turn-off point in the Σ–D relation (which is not an evolutionary track), *i.e.* after the SNR reaches a diameter of roughly about 36.5 pc the slope of the Σ–D relation sharply changes.

References

Ahumada, J. and Lapasset, E. (1995). *A&AS*, **109**, 375.
Albinson, J. S., Tuffs, R. J., Swinbank, E. and Gull, S. F. (1986). *MNRAS*, **219**, 427.
Allakhverdiev, A. O., Amnuel, P. R., Guseinov, O. H. and Kasumov, F. K. (1983a). *Ap&SS*, **97**, 261.
Allakhverdiev, A. O., Amnuel, P. R., Guseinov, O. H. and Kasumov, F. K. (1983b). *Ap&SS*, **97**, 287.
Allakhverdiev, A. O., Guseinov, O. H. and Kasumov, F. K. (1986a). *Astrofizika*, **24**, 97.
Allakhverdiev, A. O., Guseinov, O. H., Kasumov, F. K. and Yusifov, I. M. (1986b). *Ap&SS*, **121**, 21.
Allakhverdiev, A. O., Guseinov, O. H. and Kasumov, F. K. (1986c). *Astrofizika*, **24**, 397.
Allakhverdiev, A. O., Asvarov, A. I., Guseinov, O. H. and Kasumov, F. K. (1986d). *Ap&SS*, **123**, 237.
Allakhverdiev, A. O., Alpar, M. A., Gök, F. and Guseinov, O. H. (1997). *Tur. Jour. of Phys.*, **21**, 688.
Allen, G. E., Petre, R. and Gotthelf, E. V. (1998). *AAS*, **193**, 5101.
Ankay, A. and Guseinov, O. H. (1998). *A&ATr*, **17**, 301.
Asaoka, I. and Aschenbach, B. (1994). *A&A*, **284**, 573.
Asvarov, A. I., Dogiel, V. A., Guseinov, O. H., Kasumov, F. K. (1990). *A&A*, **229**, 196.
Aydin, C., Albayrak, B., Ankay, A. and Guseinov, O. H. (1997). *Tr. J. of Physics*, **21**, 857.
Bamba, A., Koyama, K. and Tomida, H. (2000). *PASJ*, **52**, 1157.
Bandiera, R. (1987). *ApJ*, **319**, 885.
Bandiera, R., Pacini, F. and Salvati, M. (1996). *ApJ*, **465**, L39.
Becker, W., Brazier, K., Trumper, J. (1996). *A&A*, **306**, 464.
Becker, R. H., Helfand, D. J. and Szymkowiak, A. E. (1982). *ApJ*, **255**, 557.
Bell, A. R. (1978a). *MNRAS*, **182**, 147.
Bell, A. R. (1978b). *MNRAS*, **182**, 443.
Berdnikov, L. N. and Efremov, Y. N. (1993). *Pisma Astronomicheskii Zhurnal*, **19**, 957.
Berkhuijsen, E. M. (1986). *A&A*, **166**, 257.
Berthiaume, G. D., Burrows, D. N., Garmire, G. P. and Nousek, J. A. (1994). *ApJ*, **425**, 132.
Blaha and Humphreys (1989). *AJ*, **98**, 1598.
Blair, W. P., Sankrit, R., Raymond, J. C. and Long, K. S. (1999). *AJ*, **118**, 942.
Blair, W. B., Raymond, J. C. and Kriss, G. A. (1995). *ApJ*, **454**, L53.
Blandford, R. D. and Cowie, L. L. (1982). *ApJ*, **260**, 625.
Bocchino, F., Maggio, A. and Sciortino, S. (1999). *A&A*, **342**, 839.
Borkowski, K. J., Blondin, J. M. and Sarazin, C. L. (1992). *ApJ*, **400**, 222.
Borkowski, K. J., Rho, J., Reynolds, S. P. and Dyer, K. K. (2001). *ApJ*, **550**, 334.
Braun, R. (1987). *A&A*, **171**, 233.
Braun, R. and Strom, R. G. (1986). *A&A*, **164**, 208.
Braun, R., Goss, W. M. and Lyne, A. G. (1989). *ApJ*, **340**, 355.
Brazier, K. T. S. and Johnston, S. (1999). *MNRAS*, **305**, 671.
Brazier, K. T. S., Kanbach, G. and Carraminana, A. (1996). *MNRAS*, **281**, 1033.
Brazier, K. T. S., Reimer, O., Kanbach, G. and Carraminana, A. (1998). *MNRAS*, **295**, 819.
Camilo, F., Stairs, I. H., Lorimer, D. R., *et al.* (2002), astro-ph/0204219.
Carter, L. M., Dickel, J. R. and Bomans, D. J. (1997). *PASP*, **109**, 990.
Case, G. L. and Bhattacharya, D. (1998). *ApJ*, **504**, 761.
Caswell, J. L., Kesteven, M. J., Komesaroff, M. M., *et al.* (1987). *MNRAS*, **225**, 329.
Caswell, J. L., Murray, J. D., Roger, R. S., *et al.* (1975). *A&A*, **45**, 239.
Caswell, J. L. and Lerche, I. (1979). *MNRAS*, **187**, 201.
Cha, A. N., Sembach, K. R. and Danks, A. C. (1999). *ApJ*, **515**, L25.
Chakrabarty, D., Pivovaroff, M. J., Hernquist, L. E., *et al.* (2001). *ApJ*, **548**, 800.
Chevalier, R. A., Krishner, R. P. and Raymond, J. C. (1980). *ApJ*, **235**, 186.
Chevalier, R. A. (1999). *ApJ*, **511**, 798.
Clark, D. H. and Caswell, J. L. (1976). *MNRAS*, **174**, 267.
Claussen, M. J., Frail, D. A., Goss, W. M. and Gaume, R. A. (1997). *ApJ*, **489**, 143.
Claussen, M. J., Goss, W. M., Frail, D. A. and Seta, M. (1999a). *AJ*, **117**, 1387.
Claussen, M. J., Goss, W. M., Frail, D. A. and Desai, K. (1999b), *ApJ*, **522**, 349.
Cox, D. P., Shelton, R. L., Maciejewski, W., *et al.* (1999). *ApJ*, **524**, 179.
Craig, W. W., Hailey, C. J. and Pisarski, R. L. (1997). *ApJ*, **488**, 307.
Danks, A. C. (2000). *Ap&SS*, **272**, 127.

Davelaar, J., Smith, A. and Becker, R. (1986). *ApJ*, **300**, L59.
De Jager, O. C., Harding, A. K. and Strickman, M. S. (1996). *ApJ*, **460**, 729.
Denoyer, L. K. (1979a). *ApJ*, **228**, L41.
Denoyer, L. K. (1979b). *ApJ*, **232**, L165.
Denoyer, L. K. (1983). *ApJ*, **264**, 141.
Du Plessis, I., de Jager, D. C., Buchner, S., *et al.* (1995). *AJ*, **453**, 746.
Dickel, J. R., Green, A., Ye, T. and Milne, D. K. (1996). *AJ*, **111**, 340.
Dickel, J. R., Strom, R. G. and Milne, D. K. (2001). *ApJ*, **546**, 447.
Diplas, A. and Savage, B.D. (1994). *ApJS*, **93**, 211.
Dubner, G. M., Velazquez, P. F., Goss, W. M. and Holdaway, M. A. (2000). *AJ*, **120**, 1933.
Efremov, Y. N. (1989). *Ochagi zvezdoobrazovaniya v galaktikakh (Sites of star formation in galaxies)*. Nauka, Moscow.
Eikenberry, S. S. (2002). *Invited Review for the Woods Hole (2001) Conf. on. GRBs/SGRs* (astro-ph/0203054).
Favata, F., Vink, J., Dal Fiume, D., *et al.* (1997). *A&A*, **342**, L49.
Fesen, R. A. (1984). *ApJ*, **281**, 658.
Fesen, R. A., Blair, W. P., Kirshner, R. P., *et al.* (1981). *ApJ*, **247**, 148.
Fesen, R. A. and Hurford, A. P. (1995). *AJ*, **110**, 747.
Fesen, R. A., Winkler, P. F., Rathore, Y., *et al.* (1997). *AJ*, **113**, 767.
Fesen, R. A., Wu, C.-C., Leventhal, M. and Hamilton, A. J. S. (1988). *ApJ*, **327**, 164.
Fesen, R. A., Downes, R. A. and Wallace, D. (1995). *AJ*, **110**, 2876.
Fich, M. (1986). *ApJ*, **303**, 465.
Fink, H. H., Asaoka, I., Brinkmann, W., Kawai, N. and Koyama, K. (1994). *A&A*, **283**, 635.
Frail, D. A., Goss, W. M., Reynoso, E. M., *et al.* (1996). *AJ*, **111**, 1651.
Frail, D. A., Goss, W. M. and Slysh, V. I. (1994a). *ApJ*, **424**, L111.
Frail, D. A., Kassim, N. E. and Weiler, K. W. (1994b). *AJ*, **107**, 1120.
Frail, D. A., Kassim, N. E., Cornwell, T. J. and Goss, W. M. (1995). *ApJ*, **454**, L129.
Frail, D. A. and Kulkarni, S. R. (1991). *Nature*, **352**, 785.
Frail, D. A. and Moffett, D. A. (1993). *ApJ*, **408**, 637.
Fujimoto, R., Tanaka, Y., Inoue, H., *et al.* (1995). *PASJ*, **47**, L31.
Furst, E., Reich, W. and Seiradakis, J. H. (1993). *A&A*, **276**, 470.
Gaensler, B. M., Gotthelf, E. V. and Vasisht, G. (1999a). *ApJ*, **526**, L37.
Gaensler, B. M., Brazier, K. T. S., Manchester, R. N. (1999b). *MNRAS*, **305**, 724.
Gaensler, B. M. (2000). *Pulsar Astronomy-(2000) and Beyond, ASP Conference.* Series, Vol. 202, p. 703.
Gaensler, B. M., Dickel, J. R. and Green, A. J. (2000a). *ApJ*, **542**, 380.
Gaensler, B. M., Bock, D. C. -J. and Stappers, B. W. (2000b). *ApJ*, **537**, L35.
Galas, C. M. F., Tuohy, I. R. and Garmire, G. P. (1980). *ApJ*, **236**, L13.
Galas, C. M., Tuohy, I. R. and Garmire, G. P. (1980). *ApJ*, **119**, 281.
Garmany, C. D. and Stencel, R. E. (1992). *A&AS*, **94**, 211.
Giacani, E. B., Dubner, G. M., Kassim, N. E., *et al.* (1997). *AJ*, **113**, 1379.
Giacani, E. B., Dubner, G. M., Green, A. J., Goss, W. M. and Gaensler, B. M. (2000). *AJ*, **119**, 281.
Ginzburg, V. L. (1981). *Teoreticheskaya fizika i astrofizika, Izd.* Nauka, Moscow.
Gotthelf, B. V. and Vasisht, G. (1998). *NewA*, **3**, 293.
Gotthelf, E. V., Vasisht, G. and Dotani, T. (1999a). **522**, L49.
Gotthelf, E. V., Petre, R. and Vasisht, G. (1999b). *ApJ*, **514**, L107.
Gotthelf, E. V., Petre, R. and Hwang, U. (1997). *ApJ*, **487**, L175.
Gray, A. D., Landecker, T. L., Dewdney, P. E. and Taylor, A. R. (1999). *ApJ*, **514**, 221.
Green, D. A. (1984). *MNRAS*, **209**, 449.
Green, D. A. (1989). *MNRAS*, **238**, 737.
Green, D. A. (2000). *A Catalogue of Galactic Supernova Remnants* (2000 August version).
Green, D. A. (2001). *A Catalogue of Galactic Supernova Remnants* (2001 December version), http://www.mrao.cam.ac.uk/surveys/snrs/
Greidanus, H. and Strom, R. G. (1992). *A&A*, **257**, 265.
Greiveldinger, C., Caucino Massaglia, S., *et al.* (1995). *ApJ*, **454**, 855.
Guo, Z. and Burrows, D. N. (1997). *ApJ*, **480**, L51.
Guseinov, O. H., Yerli, S. K., Özkan, S., Sezer, A. and Tagieva, S. O. (2002). preprint.
Hailey, C. J. and Craig, W. W. (1994). *ApJ*, **434**, 635.
Hamilton, A. J., Fesen, R. A., Wu, C. C., *et al.* (1997). *ApJ*, **482**, 838.
Helfand, D. J., Becker, R. H. and White, R. L. (1995). *ApJ*, **453**, 741.
Huang, Y.-L. and Thaddeus, P. (1985). *ApJ*, **295**, L13.
Huang, Y.-L. and Thaddeus, P. (1986). *ApJ*, **309**, 804.
Hughes, J. P., Helfand, D. J. and Kahn, S. M. (1984). *ApJ*, **281**, L25.
Hulleman, F., van Kerkwijk, M. H., Verbunt, F. W. M. and Kulkarni, S. R. (2000). *A&A*, **358**, 605.
Humphreys, R. M. (1978). *A&AS*, **38**, 309.
Hwang, U., Petre, R. and Hughes, J. P. (1999). *AAS*, **194**, 8513.
Israel, F. P. (1980). *A&A*, **90**, 246.
Junkes, N., Furst, E. and Reich, W. (1992). *A&AS*, **96**, 1.

Kahn, S. M., Gorenstein, P., Harnden, F. R., Jr. and Seward, F. D. (1985). *ApJ*, **299**, 821.
Kaplan, D. L., Kulkarni, S. R. and Murray, S. S. (2001). *arXiv:astro-ph/0102054v3*.
Kaspi, V. M., Chakrabarty, D. and Steinberger, J. (1999). *ApJ*, **525**, L33.
Kaspi, V. M., Manchester, R. N., Johnston, S., *et al.* (1996). *AJ*, **111**, 2028.
Kaspi, V. M., Lyne, A. G., Manchester, R. N., *et al.* (1993). *ApJ*, **409**, L57.
Kaspi, V. M. (2000). In: Kramer, M, Wek, N. and Wielebinski, N. (Series Eds.), *Pulsar Astronomy-(2000) and beyond. ASP Conference*, p. 485.
Kellett, B. J., Branduardi-Raymont, G., Gulhane, J. L., *et al.* (1987). *MNRAS*, **225**, 199.
Keohane, J., Petre, R., Gotthelf, E. V., *et al.* (1997). *ApJ*, **484**, 350.
Kirshner, R. P., Winkler, P. F. and Chevalier, R. A. (1987). *ApJ*, **315**, L135.
Koralesky, B., Frail, D. A., Goss, W. M., Claussen, M. J. and Green, A. J. (1998a). *AJ*, **116**, 1323.
Koralesky, B., Rudnick, L., Gotthelf, E. V. and Keohane, J. W. (1998b). *ApJ*, **505**, L27.
Koyama, K., Petre, R., Gotthelf, E. V., *et al.* (1995). *Nature*, **378**, 255.
Krymsky, G. F. (1977). *Dokl. Akad. Nauk SSSR*, **234**, 1306.
Laming, J. M., Raymond, J. C., McLaughlin, B. M. and Blair, W. P. (1996). *ApJ*, **472**, 267.
Landecker, T. L., Pineault, S., Routledge, D. and Vaneldik, J. F. (1989). *MNRAS*, **237**, 277.
Landecker, T. L., Roger, R. S. and Higgs, L. A. (1980). *A&AS*, **39**, 133.
Landecker, T. L., Routledge, D., Reynolds, S. P., *et al.* (1999). *ApJ*, **527**, 866.
Li, Z. W. and Wheeler, J. C. (1984). *BAAS*, **16**, 334.
Long, K. S., Blair, W. P., White, R. L. and Matsui, Y. (1991). *ApJ*, **373**, 567.
Long, K. S., Blair, W. P. and van den Bergh, S. (1988). *ApJ*, **333**, 749.
Long, K. S. and Blair, W. P. (1990). *ApJ*, **358**, L13.
Lorimer, D. R., Lyne, A. G. and Camilo, F. (1998). *A&A*, **331**, 1002.
Lozinskaya, T. A. (1981). *Soviet Astron. Lett.*, **7**, 17.
Lozinskaya, T. A., Pravdikova, V. V., Finoguenov, A. V., *et al.* (2000). *AstL*, **26**, 77.
Lyne, A. G., Pritchard, R. S., Graham-Smith, F. and Camilo, F. (1996). *Nature*, **381**, 497.
Lynga, G. (1987). *Catalogue of Open Clusters*, 5th edn, Lund Observatory.
Marsden, D., Lingenfelter, R., Rothschild, R. and Higdon, J. (1999). *AAS*, 195, 26.05 (astro-ph/9912315).
Mavromatakis, F., Papamastorakis, S., Paleologou, E. V. and Ventura, J. (2000). *A&A*, **353**, 371.
Meaburn, J. and Allan, P. M. (1986). *MNRAS*, **222**, 593.
Melnik, A. M. and Efremov, Yu. N. (1995). *AstL*, **21**, 10.
Mereghetti, S., Bignami, G. F. and Caraveo, P. A. (1996). *ApJ*, **464**, 842.
Mills, B. Y., Turtle, A. J., Little, A. G. and Durdin, J. M. (1984). *Austral. J. Phys.*, **37**, 321.
Milne, D. K. (1979). *Australian J. Phys.*, **32**, 83.
Minkowski, R. (1958). *Rev. Mod. Phys.*, **30**, 1048.
Morini, M., Robba, N. R., Smith, A. and Van der klis, M. (1988). *ApJ*, **333**, 777.
Murray, S. S., Ransom, S. M., Juda, M., *et al.* (2002). *ApJ*, **566**, 1039.
Neckel, Th. and Klare, G. (1980). *A&AS*, **42**, 251.
Nugent, J., Pravdo, S., Garmire, G., *et al.* (1984). *ApJ*, **284**, 612.
Odegard, N. (1986). *ApJ*, **301**, 813.
Ögelman, H. and Buccheri, R. (1987). *A&A*, **186**, L17.
Ögelman, H., Koch-Miramond, L. and Auriere, M. (1989). *ApJ*, **342**, L83.
Olbert, C. M., Clearfield, C. R., Williams, N. E., *et al.* (2001). *ApJ*, **554**, L205.
Oliva, E., Moorwood, A. F. M. and Danziger, I. J. (1990). *A&A*, **240**, 453.
Oliva, E., Moorwood, A. F. M., Drapatz, S., *et al.* (1999). *A&A*, **343**, 943.
Parmar, A. N., Oosterbroek, T., Favata, F., *et al.* (1998). *A&A*, **330**, 175.
Patel, S. K., Kouveliotou, C., Woods, P. M., *et al.* (2001). *ApJ*, **563**, L45.
Pavlov, G. G., Zavlin, V. E. and Trumper, J. (1999). *ApJ*, **511**, L45.
Petre, R., Becker, C. M. and Winkler, P. F. (1996). *ApJ*, **465**, L43.
Petruk, O. (1999). *A&A*, **346**, 961.
Pfeffermann, E., Aschenbach, B. and Predehl, P. (1991). *A&A*, **246**, L28.
Phillips, A. P., Gondhalekar, P.M. and Blades, J. C. (1981). *MNRAS*, **195**, 485.
Pineault, S., Landecker, T. L., Madore, B. and Gaumont-Guay, S. (1993). *AJ*, **105**, 1060.
Pineault, S., Landecker, T. L. and Routledge, D. (1987). *ApJ*, **315**, 580.
Poveda, A. and Woltjer, L. (1968). *AJ*, **73**, 65.
Predehl, P. and Trumper, J. (1994). *A&A*, **290**, L29.
Radhakrishnan, V., Goss, W. M., Murray, J. D. and Brooks, J. W. (1972). *ApJS*, **24**, 49.
Raymond, J. C., Blair, W. P., Long, K. S., *et al.* (1997). *ApJ*, **482**, 881.
Reach, W. T. and Rho, J. (1998). *ApJ*, **507**, L93.
Reed, J. E., Hester, J. J., Fabian, A. C. and Winkler, P. F. (1995). *ApJ*, **440**, 706.
Reich, W. and Braunsfurth, E. (1981). *A&A*, **99**, 17.
Reich, W., Furst, E. and Arnal, E. M. (1992). *A&A*, **256**, 214.
Reynolds, S. P., Lyutikov, M., Blandford, R. D. and Seward, F. D. (1994). *MNRAS*, **271**, L1.
Reynolds, S. P. (1996). *ApJ*, **459**, L13.
Reynoso, E. M., Dubner, G. M., Goss, W. M. and Arnal, E. M. (1995). *AJ*, **110**, 318.
Reynoso, E.M. Moffett, D. A., Goss, W. M., *et al.* (1997). *ApJ*, **491**, 816.

Reynoso, E. M., Velazquez, P. F., Dubner, G. M. and Goss, W. M. (1999). *AJ*, **117**, 1827.
Reynoso, E. M. and Goss, W. M. (1999). *AJ*, **118**, 926.
Rho, J. and Petre, R. (1996). *ApJ*, **467**, 698.
Rho, J. and Petre, R. (1997). *ApJ*, **484**, 828.
Rho, J. and Petre, R. (1998). *ApJ*, **503**, L167.
Rho, J. H., Petre, R., Schlegel, E. M. and Hester, J. (1994). *ApJ*, **430**, 757.
Rho, J., Decourchelle, H. and Petre, H. (1998). *AAS*, **193**, 7401.
Rho, J. H. and Petre, R. (1993). *American Astronomical Society Meeting*, **183**, 101.07.
Rho, J.-H., Petre, R., Pisarski, R. and Jones, L. R. (1996). Max-Planck Institut fur Extraterres. *Trische Physik report 1996*, **263**, 273.
Rho, J., Jarrett, T. H., Cutri, R. M. and Reach, W. T. (2001). *ApJ*, **547**, 885.
Roberts, D. A., Goss, W. M., Kalberla, P. M. W., *et al.* (1993). *A&A*, **274**, 427.
Roberts, M. S. E., Kaspi, V. M., Vasisht, G. *et al.* (2000). *AA Society, HEAD,* **32**, 4411.
Roberts, M. S. E., Romani, R. W., Kawaii, N., *et al.* (2001). In: Carraminana, A., Reimer, O. and Thompson, D. J. (Eds.), *The Nature of Unidentified Galactic High Energy Gamma-Ray Sources*, Vol. 267. Kluwer Academic Publishers, Dordrecht, p. 135.
Roger, R. S., Milne, D. K., Kesteven, M. J., Wellington, K. J. and Haynes, R. F. (1988). *ApJ*, **332**, 940.
Rosado, M., Ambrocio-Cruz, P., Le Coarer, E. and Marcelin, M. (1996). *A&A*, **315**, 243.
Routledge, D., Landecker, T. L. and Vaneldik, J. F. (1986). *A&A*, **221**, 809.
Routledge, D., Dewdney, P. E., Landecker, T. L. and Vaneldik, J. F. (1991). *A&A*, **247**, 529.
Rowell, G. P., Naito, T. and Dazeley, S. A. (2000). *A&A*, **359**, 337.
Ruiz, M. T. (1983). *AJ*, **88**, 1210.
Safi-Harb, S., Ögelman, H., Finley, S. (1995). *ApJ*, **439**, 722.
Sahibov, F. H. and Smirnov, M. A. (1982). *Soviet Astron. Lett.*, **8**, 150.
Sahibov, F. H. and Smirnov, M. A. (1983). *AZh*, **60**, 676.
Schaefer, B. E. (1996). *ApJ*, **459**, 438.
Schwarz, U. J., Goss, W. M., Kalberla, P. M. and Benaglia, P. (1995). *A&A*, **299**, 193.
Seward, F. D., Harnden, F. R., Szymkowiak, A. and Swank, J. (1984). *ApJ*, **281**, 650.
Seward, F. D., Dame, T. M., Fesen, R. A. and Aschenbach, B. (1995). *ApJ*, **449**, 681.
Shklovsky, I. S. (1960). *Soviet Astron.*, **4**, 243.
Slane, P., Seward, F. D., Bandiera, R., *et al.* (1997). *ApJ*, **485**, 221.
Sollerman, J., Lundqvist, P., Lindler, D., *et al.* (2000). *ApJ*, **537**, 861.
Tagieva, S. O. (2002). accepted for publication by *Astronomy Letters.*
Tamura, K., Kawai, N., Yoshida, A. and Brinkmann, W. (1996). *PASJ*, **48**, L33.
Tatematsu, K., Fukui, Y., Landecker, T. L. and Roger, R. S. (1990). *A&A*, **237**, 189.
Taylor, J. N., Manchester, R. N., Lyne, A. G. and Camilo, F. (1996). A catalog of 706 PSRs.
Torii, K., Kinugasa, K., Katayama, K., *et al.* (1998). *ApJ*, **503**, 843.
Torii, K., Kinugasa, K., Toneri, T., *et al.* (1998). *ApJ*, **494**, L207.
Torii, K., Tsunemi, H., Dotani, T., *et al.* (1999). *ApJ*, **523**, L69.
Torii, K., Slane, P. O., Kinugasa, K., *et al.* (2000). *PASJ*, **52**, 875.
Trussoni, E., Massaglia, S., Caucino, S., *et al.* (1996). *A&A*, **306**, 581.
Tuohy, I. R. and Garmire, G. P. (1980). *ApJ*, **239**, L107.
Uyamker, B., Kothes, R. and Brunt, C. M. (2001). *Astro-ph/0110001.*
Vasisht, G., Aoki, T., Dotani, T., Kulkarni, S. R. and Nagase, F. (1996). *ApJ*, **456**, L59.
Vasisht, G. and Gotthelf, E. V. (1997). *ApJ*, **486**, L129.
Vasisht, G., Kulkarni, S. K., Anderson, S. B., *et al.* (1997). *ApJ*, **476**, L43.
Vink, G., Bloemen, H., Kasstra, J. S. and Bleeker, J. A. M. (1998). *A&A*, **339**, 201.
Weiler, K. W. and Panagia, N. (1978). *A&A*, **70**, 419.
Willingale, R., West, R. G., Pye, J. P. and Stewart, G. C. (1996). *MNRAS*, **278**, 749.
Winkler, P. F., Canizares, C. R., Clark, G. W., *et al.* (1981a). *ApJ*, **245**, 574.
Winkler, P. F., Canizares, C. R., Clark, G. W., *et al.* (1981b). *ApJ*, **246**, L27.
Winkler, P. F. and Long, K. S. (1997). *ApJ*, **491**, 829.
Woermann, B., Gaylard, M. J., Otrupcek, R., *et al.* (2000). *MNRAS*, **317**, 421.
Wooten, A. (1981). *ApJ*, **245**, 105.
Wright, M., Dickel, J., Koralesky, B. and Rudnick, L. (1999). *AJ*, **518**, 284.
Wu, C.-C., Crenshaw, D. M., Fesen, R. A., *et al.* (1993). *ApJ*, **416**, 247.
Yamauchi, S., Ueno, S., Koyama, K., *et al.* (1993). *PASJ*, **45**, 795.
Yamauchi, S., Koyama, K., Tomida, H., *et al.* (1999). *PASJ*, **51**, 13.
Zavlin, V. E., Trumper, J. and Pavlov, G. G. (1999). *ApJ*, **525**, 959.
Zavlin, V. E., Pavlov, G. G., Sanwal, D. and Trumper, J. (2000). *ApJ*, **540**, L25.